

Mimicry of High-Density Lipoprotein: Functional Peptide-Lipid Nanoparticles Based on Multivalent Peptide Constructs

Yannan Zhao,[†] Tomohiro Imura,[†] Luke J. Leman,[†] Linda K. Curtiss,[‡] Bruce E. Maryanoff,[†] and M. Reza Ghadiri^{*,†,§}

[†]Department of Chemistry, [‡]Department of Immunology and Microbial Science, and [§]The Skaggs Institute for Chemical Biology, The Scripps Research Institute, 10550 North Torrey Pines Road, La Jolla, California 92037, United States

Supporting Information

24 Pages

Experimental Procedures

Abbreviations (not defined below): BSA, bovine serum albumin; DIC, 1,3-diisopropylcarbodiimide; EDC, 1-ethyl-3-(3-dimethylaminopropyl)carbodiimide; EDTA, ethylenediamine-N,N,N',N'-tetraacetic acid; FBS, fetal bovine serum; HRP, horseradish peroxidase; LPDS, lipoprotein-deficient serum; MBHA, 4-methylbenzhydrylamine; NDGGE, nondenaturing gradient gel electrophoresis; PBS, phosphate-buffered saline; TBS, tris-buffered saline; TBST, tris-buffered-saline Tween20; TCEP, tris(2-carboxyethyl)phosphine; TES, triethylsilane; TIS, triisopropylsilane; Trt, triphenylmethyl.

Materials

Amino acids, Rink amide MBHA resin, and *N*-hydroxybenzotriazole (HOBt) were purchased from Advanced ChemTech or Nova Biochem. Other chemicals were purchased from Sigma-Aldrich or Fisher Scientific. Trifluoroacetic acid (TFA) was obtained from Halocarbon Products (Hackensack, NJ). *L*- α -Dimyristoylphosphatidylcholine (DMPC) was purchased from Avanti Polar Lipids, Inc. (Birmingham, AL). Sandoz and 8-(4-chlorophenylthio)-adenosine-3',5'-cyclic monophosphate (CPT-cAMP) were purchased from Sigma-Aldrich. Human Ac-LDL was purchased from Biomedical Technologies, Inc. Human apolipoprotein A-I (apoA-I) was purchased from Intracel Resources. HRP-conjugated goat anti-human apoA-I antibody was from Academy Bio-Medical (#11H-G1a), rabbit anti-mouse apoA-I antibody was from Meridian Life Science, and HRP-conjugated anti-rabbit IgG was from Thermo. Human plasma was obtained from normal healthy donors through The Scripps Research Institute Normal Blood Donor Program. Mouse serum samples were obtained from the Department of Animal Resources at The Scripps Research Institute.

Preparation of thioester-modified molecular scaffolds (Figure S2)

Di-*tert*-butyl 2,2'-(succinylbisglycine) (1, Figure S2).

Succinic acid (354 mg, 3.0 mmol) and *i*-Pr₂NEt (1.6 ml, 9.0 mmol) were dissolved in CH₂Cl₂ (15 mL) with stirring at 22 °C. HOBt·H₂O (1.07 g, 7.0 mmol) and EDC·HCl (1.44 g, 7.5 mmol) were added to the solution, followed by the addition of H-Gly-OtBu·HCl (1.17 g, 7.0 mmol). After stirring at 22 °C for 3 h, CH₂Cl₂ (40 mL) was added to the slightly turbid solution, and the mixture was washed three times with saturated NaHCO₃, three times with 5% KHSO₄, and once with brine. The organic layer was dried over MgSO₄. Filtration and removal of solvent gave **1** as a white solid (970 mg, 2.82 mmol) in 94% yield.

¹H NMR (400 MHz, CDCl₃): δ 6.49 (m, 2H), 3.95 (d, 4H), 2.61 (s, 4H), 1.48 (s, 18H). ESI-MS (*m/z*) 345.2014 [M+H]⁺ (MW_{calcd} = 345.2020).

Dimer scaffold, di-*N*-acetylcysteamine 2,2'-(succinylbisglycine) (2, Figure S2).

Compound **1** (950 mg, 2.76 mmol) was dissolved in 9:1 TFA/TES (20 mL) and stirred at 22 °C overnight, after which the solvent was removed by evaporation. CH₂Cl₂ was added to the residue and removed under vacuum to remove traces of TFA. The crude white solid thus obtained was dissolved in CH₂Cl₂ (15 mL) and *i*-Pr₂NEt (1.6 ml, 9.0 mmol) was added. HOBt·H₂O (1.07 g, 7.0 mmol) and EDC·HCl (1.44 g, 7.5 mmol) were added to the solution, followed by the addition of *N*-acetylcysteamine (744 mg, 7.0 mmol). After stirring for 10 min, the solution had turned cloudy. DMF (2 mL) was added to solubilize the reaction, but the solution remained cloudy. After 2 h, the solid that had formed during the reaction was collected by filtration and washed with CH₂Cl₂ and EtOAc. The solid was dried under vacuum to yield **2** (822 mg, 1.89 mmol) in 68% yield.

¹H NMR (500 MHz, DMSO-*d*₆): δ 8.66 (m, 2H), 8.09 (m, 2H), 4.03 (d, 4H), 3.19 (q, 4H), 2.94 (t, 4H), 2.50 (s, 4H), 1.85 (s, 6H). ESI-MS (*m/z*) 435.1379 [M+H]⁺ (MW_{calcd} = 435.1366).

Tri-*tert*-butyl 2,2',2''-(benzenetricarboxyltrisglycine) (3, Figure S2).

1,3,5-Benzenetricarboxylic acid (420 mg, 2.0 mmol) and *i*-Pr₂NEt (1.6 ml, 9.0 mmol) were dissolved in 3:1 CH₂Cl₂/DMF (30 mL) and stirred at 22 °C. EDC·HCl (1.19 g, 6.2 mmol) and HOBt·H₂O (0.95 g, 6.2 mmol) were added to the solution, followed by the addition of H-Gly-OtBu·HCl (1.08 g, 6.4 mmol). After stirring at 22 °C for 24 h, the initially cloudy had turned clear. CH₂Cl₂ (50 mL) was added to the solution, and the mixture was washed three times with saturated NaHCO₃, three times with 5% KHSO₄, and once with brine. The organic layer was dried over MgSO₄. After purification by flash chromatography (1:1 EtOAc/hexanes), **3** was obtained as a white solid (500 mg, 0.91 mmol) in 46% yield.

¹H NMR (500 MHz, CDCl₃): δ 8.24 (s, 3H), 8.03 (m, 3H), 4.17 (d, 6H), 1.58 (s, 27H). ESI-MS (*m/z*) 550.2751 [M+H]⁺ (MW_{calcd} = 550.2759).

Trimer scaffold, tri-*N*-acetylcysteamine 2,2',2''-(benzenetricarboxyltrisglycine) (4, Figure S2).

Compound **3** (480 mg, 0.87 mmol) was dissolved in 9:1 TFA/TES (20 mL) and stirred at 22 °C for 2 h, after which the solvent was removed by evaporation. CH₂Cl₂ was added to the residue and removed under vacuum to remove traces of TFA. The crude white solid thus obtained was dissolved in CH₂Cl₂ (15 mL) and *i*-Pr₂NEt (1.6 ml, 9.0 mmol) was added. HOBt·H₂O (603 mg, 3.9 mmol) and EDC·HCl (757 mg, 3.9 mmol) were added to the solution, followed by the addition of *N*-acetylcysteamine (436 mg, 4.1 mmol). After stirring overnight, CH₂Cl₂ (50 mL) was added to the solution, and the mixture was washed three times with saturated NaHCO₃, three times with 5% KHSO₄, and once with brine. The product partitioned into the aqueous phase, so the combined aqueous layers were acidified to pH 3, evaporated to ~20 mL, and filtered. The aqueous solution was purified by preparative HPLC, and the product was lyophilized to yield **4** (280 mg, 0.41 mmol) as a white solid in 47% yield.

¹H NMR (500 MHz, DMSO-*d*₆): δ 9.57 (t, 3H), 8.64 (s, 3H), 8.10 (t, 3H), 4.30 (d, 6H), 3.23 (q, 6H), 2.98 (t, 6H), 1.84 (s, 9H). ESI-MS (*m/z*) 685.1791 [M+H]⁺ (MW_{calcd} = 685.1779).

Tetra-*tert*-butyl 2,2',2'',2'''-(succinylbis(azanetriyl))tetraacetate (5, Figure S2).

Succinic acid (236 mg, 2.0 mmol) and *i*-Pr₂NEt (0.8 ml, 4.5 mmol) were dissolved in CH₂Cl₂ (15 mL) and stirred at 22 °C. HOBt·H₂O (643 mg, 4.2 mmol) and EDC·HCl (844 mg, 4.4 mmol) were added to the solution, followed by the addition of di-*tert*-butyl iminodiacetate (1.03 g, 4.2 mmol). After stirring at 22 °C for 22 h, CH₂Cl₂ (40 mL) was added to the solution, and the mixture was washed three times with saturated NaHCO₃, two times with 5% KHSO₄, and once with brine. The organic layer was dried over MgSO₄ and evaporated. The product was recrystallized from Et₂O over two days at 4 °C (1:1 EtOAc/hexanes), giving **5** (537 mg, 0.94 mmol) in 47% yield.

¹H NMR (400 MHz, CDCl₃): δ 4.07 (d, 8H), 2.71 (s, 4H), 1.48 (d, 36H). ESI-MS (*m/z*) 572.53 [M+H]⁺ (MW_{calcd} = 572.69).

Tetramer scaffold, tetra-*N*-cysteaminyglycine 2,2',2'',2'''-(succinylbis(azanetriyl)) tetraacetate (6, Figure S2).

Compound **5** (374 mg, 0.65 mmol) was dissolved in 9:1 TFA/TES (5 mL) and stirred at 22 °C for 1 h, after which the solvent was removed by evaporation. CHCl₃ was added to the residue and removed under vacuum to remove traces of TFA. The crude white solid thus obtained was dissolved in CH₂Cl₂ (10 mL) and *i*-Pr₂NEt (0.45 ml, 2.6 mmol) was added. HOBt·H₂O (418 mg, 2.7 mmol) and EDC·HCl (548 mg, 2.9 mmol) were added to the solution, followed by the addition of H-Gly-OtBu·HCl (458 mg, 2.7 mmol). The mixture was slightly turbid. After stirring overnight, CH₂Cl₂ (50 mL) was added to the solution, and the mixture was washed three times with saturated NaHCO₃, three times with 5% KHSO₄, and once with brine. The product tetra-*tert*-butyl ester (419 mg, 0.52 mmol, 80% yield, ESI-MS (*m/z*) 800.69 [M+H]⁺ (MW_{calcd} = 800.89)) was used directly in the next step without further purification. The tetra-*tert*-butyl ester described above was dissolved in 9:1 TFA/TES (5 mL) and stirred at 22 °C for 2 h, after which the solvent was removed by evaporation. CH₂Cl₂, H₂O, and MeOH were added to the residue and removed under vacuum to remove traces of TFA. The crude brown foam thus obtained (140 mg, 0.24 mmol) was dissolved in CH₂Cl₂ (5 mL) and *i*-Pr₂NEt (0.24 mL, 1.39 mmol) was added. HOBt·H₂O (161 mg, 1.05 mmol) and EDC·HCl (201 mg, 1.05 mmol) were added to the solution, followed by the addition of *N*-acetylcysteamine (117 mg, 1.1 mmol). DMF (3 mL) was added to the mixture, which contained a brown precipitate, and the solution was sonicated for ~30 until the precipitate dissolved. After stirring 40 h, the solvent was evaporated under vacuum and the residue was purified using preparative HPLC and lyophilized to give compound **6** as a white solid (61 mg, 0.06 mmol) in 26% yield.

¹H NMR (500 MHz, DMSO-*d*₆): δ 9.26 (t, 2H), 8.84 (t, 2H), 8.10 (m, 4H), 4.07–4.26 (m, 16H), 3.21 (m, 8H), 2.96 (m, 8H), 2.63 (s, 4H), 1.85 (s, 12H). ESI-MS (*m/z*) 981.2902 [M+H]⁺ (MW_{calcd} = 981.2933).

Solid-phase peptide synthesis (SPPS)

Peptides were synthesized by using standard Fmoc chemistry with an Advanced Chemtech Apex 396 peptide synthesizer. A typical synthesis was performed on 0.09 mmol scale using 0.6 mmol/g Rink amide MBHA resin (Novabiochem) for preparation of a C-terminal amide. Standard side chain protecting groups included Cys(Trt), Gln(Trt), Lys(Boc), Thr(*t*Bu), Trp(Boc), Glu(OtBu), Ser(*t*Bu). Chain elongations were achieved using DIC and HOBt in NMP (*N*-methylpyrrolidinone) with 90-min couplings. Fmoc deprotection was achieved using 30% piperidine in NMP. Peptides were cleaved from the resin with concomitant side chain deprotection by agitation in a solution of 94:2.5:2.5:1 TFA/ethanedithiol/TIS/water for 3 h. The peptide was precipitated with ether, centrifuged, and washed three additional times with ether. The crude peptides were purified by preparative reverse-phase (RP)-HPLC on a Vydac 218TP C18 or 214TP C4 column. Purity was confirmed by analytical RP-HPLC. Purified peptides were characterized by analytical HPLC and MALDI-TOF mass spectrometry. Analytical reverse-phase HPLC was performed using a Vydac 214TP C-4 column or a Zorbax 300-SB C-18 column connected to a Hitachi D-7000 HPLC system. Binary gradients of solvent A (99% H₂O, 0.9% acetonitrile, 0.1% TFA) and solvent B (90% acetonitrile, 9.9% H₂O, 0.07% TFA) were employed for HPLC.

Monomeric peptide

The sequence of monomer₂₃ peptide is Cys-Gly-Val-Leu-Glu-Ser-Phe-Lys-Ala-Ser-Phe-Leu-Ser-Ala-Leu-Glu-Glu-Trp-Thr-Lys-Lys-Leu-Gln-CONH₂. MALDI-TOF MS: 2616.6 [M+H]⁺ (MW_{calcd} 2614.0). The sequence of monomer₁₆ peptide is Cys-Gly-Ser-Phe-Leu-Ser-Ala-Leu-Glu-Glu-Trp-Thr-Lys-Lys-Leu-Gln-CONH₂. MALDI-TOF MS: 1841.6 [M+H]⁺ (MW_{calcd} 1839.1).

Representative alkylation for monomer₂₃ peptide: The purified peptide (5.5 mg, 1.69 μmol) was alkylated by mixing with iodoacetamide (36.8 mg, 0.2 mmol) in 6.9 mL of 200 mM ammonium bicarbonate (NH₄HCO₃) buffer (pH 7.5) containing 14.5 mM TCEP (28.6 mg, 0.1 mmol). After 5 min, ~0.3 mL of TFA was added to quench the reaction. The product was purified by RP-HPLC. MALDI-TOF MS: 2671.1 [M+H]⁺ (MW_{calcd} 2674.8). The concentration of monomeric peptides was determined by ultraviolet absorbance ($\epsilon_{280} = 5,500 \text{ M}^{-1} \text{ cm}^{-1}$).

Native chemical ligation (NCL)

All peptide ligation reactions were performed in 200 mM 3-(*N*-morpholino)propanesulfonic acid (MOPS) buffer containing 7 M guanidine hydrochloride (Gdn·HCl), 100 mM (TCEP), pH 7.5, at room temperature. Addition of sodium ascorbate (50 mM) was found to lessen a side reaction resulting in desulfurization of the cysteine residue. Isolated yields of peptide after HPLC purification were 60–90%.

Representative NCL reaction for dimer₂₃: dimer scaffold **2** (0.74 mg, 1.70 μmol) and unalkylated monomer₂₃ peptide (15 mg, 4.59 μmol) were mixed in 1.1 mL of buffer. After 6 h, the reaction mixture was diluted to 13 mL with 200 mM NH₄HCO₃ buffer (pH 7.5) containing 50 mM iodoacetamide (120 mg, 0.65 mmol). After 5 min, ~0.3 mL of TFA was added to quench the reaction. The product was purified by RP-HPLC. MALDI-TOF MS: 5542.2 [M+H]⁺ (MW_{calcd} 5538.3). The concentration of dimeric peptides was determined by ultraviolet absorbance ($\epsilon_{280} = 11,000 \text{ M}^{-1} \text{ cm}^{-1}$).

Representative NCL reaction for trimer₂₃: trimer scaffold **4** (0.78 mg, 1.15 μmol) and peptide (15 mg, 4.59 μmol) were mixed in 0.76 mL of buffer. After 6 h, the reaction mixture was diluted to 13 mL with 200 mM NH₄HCO₃ buffer (pH 7.5) containing 50 mM iodoacetamide (120 mg, 0.65 mmol). After 5 min, ~0.3 mL of TFA was added to quench the reaction. The product was purified by RP-HPLC. MALDI-TOF MS: 8334.7 [M+H]⁺ (MW_{calcd} 8340.5). The concentration of trimeric peptides was determined by ultraviolet absorbance ($\epsilon_{280} = 16,500 \text{ M}^{-1} \text{ cm}^{-1}$).

Representative NCL reaction for tetramer₂₃: tetramer scaffold **2** (0.9 mg, 0.92 μmol) and peptide (15 mg, 4.59 μmol) were mixed in 0.92 mL of buffer. After 6 h, the reaction mixture was diluted to 13 mL with 200 mM NH₄HCO₃ buffer (pH 7.5) containing 50 mM iodoacetamide (120 mg, 0.65 mmol). After 5 min, ~0.3 mL of TFA was added to quench the reaction. The product was purified by RP-HPLC. MALDI-TOF MS: 11192.0 [M+H]⁺ (MW_{calcd} 11188.8). The concentration of tetrameric peptides was determined by ultraviolet absorbance ($\epsilon_{280} = 22,000 \text{ M}^{-1} \text{ cm}^{-1}$).

Preparation of labeled peptide constructs

Purified monomer or multivalent peptide constructs were prepared as described above, but without alkylation prior to HPLC purification. To prepare the fluorescein-labeled 23-mer family of peptides, the peptide construct (2 μmol helical content) was dissolved in 5 mL PBS containing 4 mM TCEP at pH 7.5., a 10-fold molar excess of 5-iodoacetamidfluorescein (5-IAF, Invitrogen; 0.4 mL of 50 mM stock solution in DMF) relative to total thiols present was added dropwise. To prepare the biotin-labeled 16-mer family of peptides, the peptide construct (5 μmol helical content) was dissolved in 50 mL MOPS buffer containing 10 mM TCEP at pH 7.5. To this solution, a 5-fold molar excess of iodoacetyl LC biotin (Soltec Ventures; 1 mL of 25 mM stock solution in DMSO) relative to total thiols present was added dropwise. Acetonitrile (~5 mL) was added to keep the 16mer reaction solution clear. The reaction tubes were covered by aluminum foil to protect from light and incubated for 2 h at room temperature. TFA (0.1-0.2 mL) was added to quench the reaction. The products (one fluorophore per helix) were purified by RP-HPLC. Extinction coefficients for the 5-IAF-labeled constructs were calculated as described by the manufacturer (http://www.thermo.fi/eThermo/CMA/PDFs/Articles/articles_File_8081.pdf); these extinction coefficients were calculated to be monomer₂₃ = 25,900 M⁻¹ cm⁻¹; dimer₂₃ = 51,800 M⁻¹ cm⁻¹; trimer₂₃ = 77,700 M⁻¹ cm⁻¹. Extinction coefficients for the biotin-labeled constructs were monomer₁₆ = 5,500 M⁻¹ cm⁻¹; dimer₁₆ = 11,000 M⁻¹ cm⁻¹; trimer₁₆ = 16,500 M⁻¹ cm⁻¹, and tetramer₁₆ = 22,000 M⁻¹ cm⁻¹.

Multilamellar vesicle preparation

L- α -Dimyristoylphosphatidylcholine (DMPC) was dissolved in 0.5 mL CHCl₃ in a test tube and dried into a thin film by blowing N₂ gas into the tube while vortexing. The lipid film was further dried under reduced pressure overnight in a desiccator. Multilamellar vesicles (MLVs) were obtained by suspending the dried lipids into PBS (10 mM phosphate, pH 7.4, 136 mM NaCl) with vortexing and/or sonication. MLVs were typically prepared at concentrations of 10 mM.

Nanoparticle preparation

A stock solution of peptide (2-3 mg/mL) in phosphate buffered saline (PBS, 10 mM phosphate, 136 mM NaCl, pH 7.4) was added to 10 mM DMPC multilamellar vesicles (MLVs) at a 1:10 (helix:lipid) molar ratio, and the solutions were diluted with PBS to give a final concentration of 3 mM DMPC. The solutions were vortexed for 24-48 h at 25 °C before analysis by size-exclusion chromatography and electron microscopy. For some experiments, nanoparticles were prepared at a 10-fold lower concentration, with no apparent differences in particles size or morphology. The final peptide:DMPC ratio in purified particles was determined using SEC purified nanoparticles by separately measuring the peptide concentration using UV absorbance at 280 nm and the phospholipid concentration using a commercially-available assay kit (Biovision).

Liposome clearance assay

L- α -Dimyristoylphosphatidylcholine (DMPC) multilamellar vesicles were prepared by vortexing in tris buffered saline (10 mM Tris, pH 7.4, 100 mM NaCl, 0.25 mM EDTA, 0.0005% NaN₃) for 5 minutes, and the turbid solution was then extruded at least 11 times using 200 nm pore size polycarbonate with an extruder (Avanti Polar Lipids, Inc.). Incubations with peptides were carried out at room temperature at the appropriate DMPC:peptide ratio in a 96-well plate. Turbidity was monitored at optical density (O.D.) 485 nm with a microplate reader (Genios, Tecan Instruments) using black 96-well plates.

Pyrene fluorescence measurements

The self-association of the 23-mer peptide constructs was monitored by using pyrene fluorescence at room temperature.^{S1} The characteristic intensity ratio, I_1/I_3 , was measured as a function of the peptide concentration with a Sim-Aminco Series 2 luminescence spectrometer with the AB2 (v5.5) software package (Thermo Electron). Excitation of the pyrene probe was performed at 335 nm, and the detection wavelengths were 373 nm for I_1 (first peak) and 384 nm for I_3 (third peak). The thin pyrene films were prepared by transferring a sufficient amount of a methanol-based stock solution of pyrene to test tubes and then evaporating the solvent under a stream of nitrogen. The peptide solution in tris buffered saline (25 mM tris, 150 mM NaCl, pH 7.4) was then added the tube containing the pyrene film. The final pyrene concentration was 5×10^{-7} M. The samples were incubated in the dark for 24 h at room temperature before measurements were taken.

Surface tension measurement

Surface tension measurements (γ) were carried out at 22 °C using Wilhelmy plate and a pressure sensor type PS4 (NIMA technology, Coventry, England). The peptide solutions were left at least for one day to reach equilibrium at 22 °C. Reproducibility was checked by frequent determination of the surface tension of deionized water (72 mN/m).

Size-exclusion chromatography

Samples were passed through a 0.45 μ m PVDF (polyvinylidene fluoride) filter and injected to a Superdex 200 HR 10/30 column (Amersham Biosciences, Piscataway, NJ) at room temperature at a flow rate of 0.5 mL/min using an AKTA purifier chromatography system. Tris buffered saline (10 mM Tris, pH 7.4, 100 mM NaCl, 0.25 mM EDTA, 0.0005% NaN₃) or phosphate buffered saline (10 mM phosphate, 136 mM NaCl, pH 7.4) was used as a running buffer. The void volume was at 7.1 mL. The standards were: thyroglobulin (669,000 Da, 17 nm), ferritin (440,000 Da, 12.2 nm), BSA (67,000 Da, 7.1 nm), and ribonuclease A (13,700 Da), which gave the following retention volumes (mL): 8.3, 11.0, 14.0, and 17.2, respectively.

Transmission electron microscopy (TEM)

The nanoparticle fractions collected by SEC were imaged without further purification. Glow-discharged copper grids (400 mesh) coated with carbon and formvar (G400-Cu, Electron Microscopy Sciences, Hatfield PA) were then immediately inverted, carbon surface down, onto 7 μ L droplets of sample solutions placed on Parafilm. After 3 min, excess liquid was wicked off and the grids immediately placed onto individual droplets of aqueous 2% phosphotungstic acid at pH 7.0. After 2 min, excess stain was removed and the grids were allowed to dry thoroughly. Images were taken on a Philips CM100 electron microscope (FEI, Hillsbrough OR) at 80 kV and collected using a Megaview III CCD camera (Olympus Soft Imaging Solutions, Lakewood, CO). Size measurements were made on at least 50 nanoparticles, quantified using SimpleDigitizer 3.1.8 or Photoshop CS4 software.

Circular dichroism

Circular dichroism (CD) measurements were obtained on an Aviv CD spectrometer model 62DS using a 1 nm bandwidth in 0.5 cm cells at 23 °C. Peptide nanoparticles for CD were prepared in PBS at lipid/peptide ratios of 10:1 for monomer, 20:1 for dimer, 30:1 for trimer, 40:1 for tetramer, and were purified by SEC prior to CD analysis for the 16-mer family of peptides. The peptide concentrations in the nanoparticle samples were in the

concentration range of 5–50 μM , as determined by UV absorbance at 280 nm (monomer₁₆, 12.1 μM ; dimer₁₆, 17.6 μM ; trimer₁₆, 8.0 μM ; tetramer₁₆, 5.2 μM ; monomer₂₃, 50 μM ; dimer₂₃, 25 μM ; trimer₂₃, 17 μM ; tetramer₂₃, 12.5 μM ; 4F, 50 μM). To prepare the lipid-free samples, aliquots of peptide stock solutions (~1 mg/mL in PBS) were diluted with PBS to concentrations of 5–50 μM (monomer₁₆, 10.2 μM ; dimer₁₆, 7.1 μM ; trimer₁₆, 6.4 μM ; tetramer₁₆, 4.3 μM ; monomer₂₃, 50 μM ; dimer₂₃, 25 μM ; trimer₂₃, 17 μM ; tetramer₂₃, 12.5 μM ; 4F, 50 μM). Mean residue ellipticities ($[\theta]_{\text{mr}}$) were calculated using the equation $[\theta]_{\text{mr}} = \theta_{\text{obs}} / (10 \cdot l \cdot c \cdot n)$, where θ_{obs} is the measured ellipticity in mdeg, l is the pathlength in cm, c is the concentration of peptide in M, and n is the number of amino acid residues in the construct (16 for monomer₁₆, 32 for dimer₁₆, 48 for trimer₁₆, and 64 for tetramer₁₆; 23 for monomer₂₃, 46 for dimer₂₃, 69 for trimer₂₃, and 92 for tetramer₂₃).

Analytical ultracentrifugation

Analytical ultracentrifugation (AUC) sedimentation velocity measurements were recorded for the 16-residue family of peptides on a Beckman Optima XL-I instrument employing double sector cells equipped with a sapphire optical window. Peptides were dissolved in PBS buffer at three concentrations (see Table S2 for concentrations used). The reference compartment was loaded with matching PBS. Samples (400 μL) were spun at 60,000 rpm at 20 °C with UV absorbance monitored at 280 nm and 225 nm. The data were first fit using the 'continuous c(s) distribution' direct boundary model as implemented in SEDFIT v.13.0b (www.analyticalultracentrifugation.com) to determine the overall heterogeneity of the sample and the sedimentation coefficient of the major species, from which an estimate of the molecular weight could be made (Table S2).^{S2} These analyses suggested that the multivalent peptide constructs were self-associating at the concentrations tested, whereas the monomer was not. Therefore, for each construct the data from the two higher concentration samples (recorded at 280 nm) were simultaneously fit using the 'monomer-dimer self-association' model as implemented in SEDPHAT v.10.40.^{S3} The dissociation constants (K_D) determined from these fits are given in Table S2. Similar fits using the 'monomer-trimer self-association' model gave poorer chi-squared values and calculated sedimentation coefficients that did not match the observed values as determined in the c(s) distributions. For all fits, a partial specific volume of 0.74 cm^3/g was used (calculated based on amino acid composition using SEDNTERP), and the frictional ratio was set to 1.2.

Cholesterol efflux

Our protocol was based on a reported procedure.^{S4} J774A.1 cells (TIB-67; American Type Culture Collection, Manassas, VA) were seeded in 12-well culture plate at 2×10^5 cells/mL and cultured to 80–90% confluency in DMEM (Dulbecco's Modified Eagle's Medium) with 10% FBS at 5% CO_2 . Cells were rinsed twice with DMEM and further incubated for 48 h with 40 $\mu\text{g}/\text{ml}$ acetylated low-density lipoprotein (ac-LDL, Biomedical Technologies) in presence of 2 $\mu\text{g}/\text{ml}$ Sandoz (Sigma) ACAT (acyl-CoA:cholesterol acyltransferase) inhibitor and 5% LPDS (Sigma) in DMEM. Non-incorporated lipids were removed from cells by washing twice with DMEM. The foam cells were equilibrated for 12 h in DMEM with 5% LPDS, 2 $\mu\text{g}/\text{mL}$ Sandoz ACAT inhibitor, and 0.3 mM CPT-cAMP. The efflux was initiated by the addition of peptides in DMEM. Aliquots of medium were taken at the time points indicated in the figure and centrifuged (1000 rpm, 10 min) to remove floating cells. At the end of the experiment, cell monolayers were rinsed three times with ice-cold DMEM and lysed by the addition of 200 μL Cytobuster lysis buffer. After incubation at room temperature for 10 min, cell lysates were homogenized using a homogenizer (PowerGen 125, Fisher Scientific). Cell-free medium and cell lysates were analyzed for total cholesterol amounts using a cholesterol Amplex assay kit (Invitrogen). Cholesterol efflux at each time point was calculated as from the amount of cholesterol in the medium as a percentage of the total cholesterol (medium + lysate).

Human plasma remodeling

All procedures involving human samples were approved by The Scripps Research Institute Institutional Review Board. Our protocol was based on a reported procedure.^{S5} Blood samples from normal healthy human donors were obtained from The Scripps Research Institute Normal Blood Donor Program. EDTA-anticoagulated whole blood was centrifuged at 1500 x g for 15 min within 1 h of being drawn from the donor. The plasma layer was aliquoted and used immediately or frozen at -80 °C for future use. Plasma samples (30 μL) were treated with peptide construct stocks (~1 mg/mL) prepared in PBS (10 mM phosphate, 136 mM NaCl, pH 7.4). Samples were incubated at 37 °C for various times, and then quenched by adding 270 μL of 50% sucrose (1:9 dilution). Samples were mixed with 2x native loading buffer (125 mM tris, pH 6.8, 0.02% bromophenol, 20% glycerol), of which 6 μL was loaded onto a 4–20% polyacrylamide gel. The molecular weight ladder used was High Molecular Weight Calibration Kit (Amersham Biosciences, #17-0445-01). Gels were run at constant 80 V at 4 °C for ~15 h using a Laemli buffer system (25 mM tris, 192 mM glycine, pH 8.3). Gels were then blotted onto nitrocellulose membranes (0.45 μm , Bio-Rad) at constant 30 V at 4 °C for 2 h using the Laemli buffer (no methanol). The membrane was blocked with 3% BSA in TBS (20 mM tris, 150 mM NaCl, pH 7.6) for 1 h at 23 °C, and then washed once for 10 min with TBST (20 mM tris, 150 mM NaCl, pH 7.6, 0.1% tween-20). The membrane was next incubated with 3% BSA in TBST containing a ~1:8000 dilution of HRP-conjugated goat anti-human apoA-I antibody (Academy Bio-

Medical, #11H-G1a) for 1 h at 23 °C. The membrane was extensively washed with TBST (at least 6 x 10 min), once with TBS. The membrane was incubated with ECL reagent (Thermo SuperSignal West Pico) for 5 min, and then exposed to photographic film (Kodak BioMax Light). Fluorescent images of nondenaturing gradient gels were taken using a Hitachi FMBIO II Multi-View fluorescent image scanner.

To track interactions between nanoparticle components and native HDLs, fluorescent images of nondenaturing gradient gels were taken using a Hitachi FMBIO II Multi-View fluorescent image scanner to visualize fluorescein-labeled 23-mer peptide (green channel) and RhB-labeled DMPC (red channel) before electroblotting. The biotin-labeled 16-mer multivalent peptides were visualized by blotting onto a Immobilon-P^{SQ} PVDF membrane (Millipore) at constant 30 V for 45 min at 4°C. The membrane was blocked with 5% BSA in TBS (20 mM tris, 150 mM NaCl, pH 7.6) for 1 h at 23 °C, followed by protein-free (TBS) blocking buffer (Pierce, Thermo Scientific) for 1 h at 23 °C. The membrane was next incubated with protein-free (TBS) blocking buffer containing a ~1:20,000 dilution of NeutrAvidin-HRP Conjugate (Pierce, Thermo Scientific) for 1 h at 23 °C. The membrane was extensively washed with high-salt TBST containing 0.5 M NaCl (at least 6 x 10 min), once with TBS, and imaged using ECL reagent as described above.

A dot blot control was performed using biotin-labeled 16-mer peptide nanoparticles diluted with PBS to 10, 5, and 2.5 µM concentrations of helices (the same number of biotin moieties are present for each sample at a given concentration). After wetting the Immobilon-P^{SQ} PVDF membrane with methanol, water, and Laemli buffer in that sequence, the pre-wet membrane was placed on wet filter paper. While the membrane was damp but not dry, 2 µL of the nanoparticle solution was spotted slowly onto the membrane, and dried before blocking and incubating with NeutrAvidin-HRP under the same condition as described above.

In vitro peptide stability in to mouse serum/proteases

Mouse serum samples were obtained from the Department of Animal Resources at The Scripps Research Institute. Peptides or peptide/DMPC nanoparticles were incubated at a final peptide concentration of 0.1 mg/mL at 37 °C with mouse serum, or at a final peptide concentration of 0.5 mg/mL with 20 mU/mL proteases (pronase, chymotrypsin, or thermolysin) in PBS (pH 7.4). After various incubation times, aliquots were removed. Serum samples were extracted with 1.5 volumes of acetonitrile containing 0.1% TFA and 0.2% triton X-100, centrifuged at 13,000 rpm for 10 min, and the supernatant was acidified with 0.5 volumes of 1% acetic acid. Aliquots of protease samples were mixed with 1.5 volumes of PBS containing protease inhibitors (Complete™) and acidified with 0.5 volumes of 1% acetic acid. The concentration of peptide in the sample was determined by LC-MS SIM, as described below. The LC injection volume for each acidified sample was 20 µL. Peptide susceptibility to pepsin digestion was assessed by incubating peptide/DMPC nanoparticles (0.5 mg/mL peptide) with pepsin (0.5 U/mL, as indicated in Figure S16) at 37 °C in 10% acetic acid (pH 2.2). Aliquots of samples were taken at indicated times, and the digestion was stopped by addition of pepstatin (10 µg/mL) and dilution with acetonitrile. The disappearance of peptide was monitored by LC/MS SIM.

The proteolytic stability of free human apoA-I and reconstituted HDL (rHDL) were also tested as positive controls. The rHDL was prepared by incubating free human apoA-I (0.5 mg/mL, 18 µM) and DMPC MLV (1.8 mM) at a 1:100 molar ratio with vortexing for 48 h at 25 °C. To initiate the digestion reaction, 10 µL protease (pronase, chymotrypsin, or thermolysin) solution was added to 500 µL apoA-I or rHDL (0.5 mg/mL) to give the final protease concentration at 20 mU/mL. After various incubation times, aliquots of samples were mixed with protease inhibitors (Complete™) and acidified with 1% acetic acid before HPLC injection. The concentration of intact protein remaining was determined by HPLC-UV quantitative analysis. Calibration curve was constructed by plotting the peak area (retention time 11.3 min, UV 230 nm) against different concentrations of apoA-I. The detection limit of apoA-I in the reaction solution was 2 µM.

Mouse pharmacokinetics and in vivo plasma remodeling

Pharmacokinetics. The TSRI Institutional Animal Care and Use Committee approved all experimental protocols involving live animals. Male mice (20 g) on a BALB/cByJ background were obtained from the Rodent Breeding Colony of the Department of Animal Resources at The Scripps Research Institute, and were maintained on a chow diet. Peptides were formulated with DMPC into lipid nanoparticles (1:10, helix:lipid molar ratio) as described above, and spin concentrated with a 3000 Molecular Weight Cutoff Centrifugal Filter (Millipore). Mice were fasted beginning 8 h before dosing, and continued the fast until after the 8-h time point blood draw was completed. Groups of three mice received a 75 mg/kg dose of 23-mer peptide nanoparticles or a 60 mg/kg dose of 16-mer peptide nanoparticles via intraperitoneal injection (0.3 mL). 30 or 60 µL blood was drawn from the retro-orbital sinus into a heparinized capillary tube before dosing (0 min) and at different intervals from 30 min to 24 h after dosing. Plasma was isolated immediately from the whole blood by centrifugation at 5,000 rpm for 10 minutes at 4°C. Immediately after blood collection and plasma separation, 20 µL of plasma were extracted with 30 µL of acetonitrile containing 0.1% TFA and 0.2% triton X-100. After vortexing for 30 s, the mixture was centrifuged at 13,000 rpm for 10 min at 4°C. 40 µL of supernatant was acidified with 20 µL of 1% acetic acid. Peptide levels in

the plasma sample were determined by using LC-MS SIM as described below, with a lower limit of quantification of 1.7, 0.8, 0.6, and 0.8 μM in plasma for monomer₁₆, dimer₁₆, trimer₁₆, and tetramer₁₆, respectively, and 0.5, 0.2, and 0.2 μM , for monomer₂₃, dimer₂₃, and trimer₂₃, respectively. The HPLC injection volume for each sample was 20 μL .

Pharmacokinetic parameters were calculated by fitting the peptide plasma concentration-time data by using WinNonlin. A one-compartment pharmacokinetic model with first-order elimination from the central compartment was used.

In vivo plasma remodeling. Immediately after blood collection and plasma separation, 10 μL of plasma were mixed with 90 μL of 50% sucrose (1:9 dilution), vortexed for 30 s, and stored at 4°C until all time points had been collected (samples were stored from 0–8 h). Samples were then mixed with 20 μL of 6x native loading buffer (125 mM tris, pH 6.8, 0.02% bromophenol, 20% glycerol). 6 μL of these samples were loaded onto a 4–20% polyacrylamide gel. Gels were run at constant 80 V at 4 °C for ~12 h using a Laemli buffer system (25 mM tris, 192 mM glycine, pH 8.3). Gels were then blotted onto nitrocellulose membranes (0.45 μm , Bio-Rad) at constant 30 V at 4 °C for 2 h using the Laemli buffer (no methanol). The membrane was blocked with 5% non-fat dry milk (NFDM) in TBST (20 mM tris, 150 mM NaCl, pH 7.6, 0.1% tween-20) for 1 h at 23 °C, and then washed for 10 min with TBST. The membrane was incubated with 1% NFDM in TBST containing a ~1:5,000 dilution of rabbit anti-mouse apoA-I antibody (Meridian Life Science) as primary antibody for 1 h at 23 °C. The membrane was washed with TBST (at least 6 x 10 min), and incubated with 1% NFDM containing a ~1:50,000 dilution of HRP-conjugated anti-rabbit IgG (Thermo) as secondary antibody for 1 h at 23 °C. The membrane was extensively washed with TBST (at least 6 x 10 min), and once with TBS. The membrane was incubated with ECL reagent (Thermo SuperSignal West Pico) for 5 min, and then imaged using photographic film (Kodak BioMax Light).

Rat pharmacokinetics

Sprague-Dawley (CrI:CD(SD)) male rats (~250 g) were purchased from Charles River Laboratories. Peptides were formulated with DMPC into lipid nanoparticles (1:10, helix:lipid molar ratio) as described above, and spin concentrated with a 3000 Molecular Weight Cutoff Centrifugal Filter (Millipore). Rats were fasted beginning 12 h before dosing, and continued the fast until after the 6-h time point blood draw was completed. Groups of three rats received a 30 mg/kg dose of lipidated peptide via intraperitoneal injection (2 mL). 100 μL blood was drawn from the tail vein into a heparinized capillary tube at different intervals from 1 to 24 h after dosing. Plasma was isolated immediately from the whole blood by centrifugation at 5000 rpm for 10 minutes at 4°C. Immediately after blood collection and plasma separation, 20 μL of plasma was extracted with 30 μL of acetonitrile containing 0.1% TFA and 0.2% triton X-100. After vortexing for 30 s, the mixture was centrifuged at 13000 rpm for 10 min at 4°C. 40 μL of supernatant was acidified with 20 μL of 1% acetic acid. Peptide levels in the plasma sample were determined by using LC-MS SIM as described below, with a lower limit of quantification of 0.2 μM for trimer. The HPLC injection volume for each sample was 20 μL .

Plasma cholesterol studies in LDLr-null mice. LDL receptor-deficient (LDLr^{-/-}) mice on a C57BL/6J background were initially purchased from Jackson Laboratories (Bar Harbor, ME) and were bred in house. The mice were weaned at 4 weeks of age and were fed ad libitum a standard chow diet (Harlan Teklad 7019). Mouse cohorts selected for study were between 10 and 12 weeks old when they were first fed the high fat diet (HFD), which contained 1.25% cholesterol, 15.8% fat, and no cholate (Harlan Teklad 94059). Animal care and use for all procedures was done in accordance with guidelines approved by the Institutional Animal Care and Use Committee of The Scripps Research Institute.

The trimer₂₃ peptide was formulated with DMPC as lipid nanoparticles at ~5 mg peptide/mL (0.6 mM). The purified peptide (~160 mg) was first dissolved in minimum amount of TFA, to which ~100 mL 5-fold diluted PBS (1/5X, 2 mM phosphate, 27.2 mM NaCl, pH 7.4) was added, and the pH was adjusted to 7.4 with NaOH. Peptide concentration in the stock solution was determined by measuring UV absorbance at 280 nm (0.19 mM). A solution of DMPC MLVs (57 mL, 10 mM in 1/5X PBS) was then added to the peptide stock solution (~1.6 mg/mL, 100 mL) at a 1:10 (helix:lipid) molar ratio, and the solutions were diluted with PBS (1/5X) to give final concentrations of peptide and DMPC to be ~1 mg/mL (0.12 mM) and 3.6 mM, respectively. The solutions were vigorously stirred for 24 h at 22–25 °C, freeze-dried, stored at -20 °C, and reconstituted with water (31.4 mL) to give peptide/DMPC stock solution at ~5 mg peptide/mL in PBS (10 mM phosphate, 136 mM NaCl, pH 7.4) before i.p. administration. The peptide/DMPC stock solutions used for i.p. studies was stored at -80°C, thawed, and filtered through a 0.22 μm sterile syringe filter before administration. Unilamellar vesicles (ULVs) of DMPC (200 nm diameter, obtained by extrusion) were used as vehicle controls. The DMPC ULVs (18 mM) were made by extrusion DMPC MLVs through a 200 nm filter in the Avanti mini extruder.

At the time when HFD started, trimer₂₃/DMPC nanoparticles were administered by daily i.p. injection (200 μL of 5 mg/mL solution, 1 mg/d per mouse) (n = 8) for 2 weeks in the continued presence of HFD. Mice receiving PBS (n = 7) or DMPC ULVs (18 mM) i.p. injections (n = 9) served as controls for the i.p. groups. After a two-week

treatment period, blood (200 μL) was collected after an overnight fast (14 to 16 hours) by retro-orbital puncture into a heparinized capillary tube. Plasma was separated immediately by centrifugation of the blood samples at 5,000 rpm for 10 minutes at 4°C. Plasma total cholesterol (TC) was measured using an enzymatic colorimetric method kit (Amplex® red cholesterol assay kit, No. A12216, Life Technologies) according to the manufacturer's instructions.

Pooled plasma (~200 μL total, 16-30 μL from each mouse) from the two-week blood draw was used for SEC lipoprotein fractionation. Lipoproteins were separated by using 3 Superdex 200 10/30 columns (GE Healthcare) connected in series. The plasma was centrifuged at 11,000 rpm for 10 min at room temperature to remove particulates (floating material was gently mixed into liquid before removing the supernatant for SEC injection). 200 μL of the pooled plasma was injected on the system eluted with 10 mM Tris-HCl buffer, pH 7.4, containing 1 mM EDTA and 150 mM NaCl; a flow rate of 0.5 ml/min and fraction size of 0.5 mL were used. Total cholesterol in the FPLC fractions was measured using the Amplex® red cholesterol assay kit (No. A12216, Life Technologies) according to the manufacturer's instructions.

LC-MS SIM quantitation of peptide concentration

Peptide concentrations were quantified by using reverse-phase HPLC coupled with mass spectrometry. The electrospray ionization mass spectrometry measurements were carried out in the positive ionization mode using a single quadrupole mass spectrometer (Hewlett Packard HP 1100 MSD series). 20 μL of sample were injected through a C8 reverse phase column (Zorbax 300-SB, 4.6 mm \times 150 mm, 5 μm) using a flow rate of 1.5 mL/min and binary gradients of solvent A (99% H₂O, 0.1% formic acid, 0.01% TFA) and solvent B (99% acetonitrile, 0.1% formic acid, 0.01% TFA). Mass detection was carried out in the selected ion monitoring (SIM) mode for the positive molecular ion, with the optimized fragmentor and capillary voltages of 3.2 kV and 230 V, respectively. The selected masses for monomer₂₃, dimer₂₃, and trimer₂₃ were 1336, 1385.2, and 2086, respectively, and for monomer₁₆, dimer₁₆, trimer₁₆, and tetramer₁₆ were 1879.0, 1330.3, 1504.7, and 2023.3, respectively. For quantitative calibration, standard curves were established using spiked peptides in mouse serum, EDTA anti-coagulated plasma, or PBS. The calibration curve was established using linear fitting of the data, with correlation coefficient ≥ 0.98 . The limit of detection in plasma was 1.7, 0.8, 0.6, and 0.8 μM for monomer₁₆, dimer₁₆, trimer₁₆, and tetramer₁₆, respectively, and 0.5, 0.2, and 0.2 μM , for monomer₂₃, dimer₂₃, and trimer₂₃, respectively, and in PBS was ~ 0.1 μM for all peptide samples.

Supporting References

- S1. a) Turro, N. J.; Baretz, B. H.; Kuo, P. L. *Macromolecules* **1984**, *17*, 1321-4. b) Imura, T.; Ohta, N.; Inoue, K.; Yagi, N.; Negishi, H.; Yanagishita, H.; Kitamoto, D. *Chem. Eur. J.* **2006**, *12*, 2434-2440.
- S2. Schuck, P. *Biophysical J.* **2000**, *78*, 1606-1619.
- S3. Schuck, P. *Anal. Biochem.* **2003**, *320*, 104-124.
- S4. Wool, G. D., Reardon, C. A. & Getz, G. S. *J. Lipid Res.* **2008**, *49*, 1268-1283.
- S5. Troutt, J. S. *et al. J. Lipid Res.* **2008**, *49*, 581-587.
- S6. Jayaraman, S.; Abe-Dohmae, S.; Yokoyama, S.; Cavigliolo, G. *J. Biol. Chem.* **2011**, *286*, 35610-35623, S35610/1-S35610/9.

Supporting Table and Figures

Table S1. Biophysical properties of 16-residue lipid-free peptide constructs.

construct	SEC Stokes radius (nm) ^[a]	concentration in AUC samples (μ M)	AUC weight-average sedimentation coefficient ^[b]	molecular weight (kDa) from sedimentation coefficient ^[c]	molecular weight ratio (obs/exp) ^[c]	AUC self-association K_D (μ M) ^[d]
monomer (1.9 kDa)	0.7	210	0.4	1.9	1.0	>400
		24.0	0.4	1.8	0.9	
dimer (4.0 kDa)	1.4	105	1.2	9.7, 3.5	2.4, 0.9	14.5
		14.2	1.1	6.9	1.7	
		1.7	1.1	4.9	1.2	
trimer (6.0 kDa)	1.7	69	1.5	11.7	2.0	6.3
		7.3	1.5	10.5	1.8	
		0.7	1.4	9.7	1.6	
tetramer (8.1 kDa)	1.9	52	1.5	12.4	1.5	30.2
		7.4	1.4	11.9	1.5	
		0.9	1.2	9.4	1.2	

[a] The Stokes radius of each construct was determined by comparison of its SEC retention time to a standard curve of four globular proteins. [b] The weight-average sedimentation coefficient for each sample was obtained from best fits of the sedimentation velocity data using the 'continuous c(s) distribution' direct boundary model in SEDFIT v.13.0b (Fig. S5). The resulting c(s) plots are shown in Fig. S4. The observed c(s) distributions for the multivalent constructs, having broad, concentration-dependent peaks, are indicative of reversible self-association occurring rapidly on the timescale of the sedimentation.[ref S6] On the other hand, the monomer c(s) distributions suggest that no self-association is occurring at the concentrations tested. For each multivalent construct, the range of observed c(s) peaks, and their corresponding molecular weights, suggest a molecular dimerization. [c] The c(s) distributions were transformed to a molar mass estimate for each sample using SEDFIT. If two values are shown, then two peaks were present in the c(s) distribution (see Figure S4). The MW ratio (obs/exp) corresponds to the observed AUC molecular weight divided by the molecular weight of the construct. [d] The dissociation constant for dimerization of each construct was obtained from best fits of the sedimentation velocity data using the 'monomer-dimer self-association' model in SEDPHAT v.10.40. Similar attempts to fit the data using the 'monomer-trimer self-association' model gave poorer chi-squared values and calculated sedimentation coefficients that did not match those determined in the c(s) distributions.

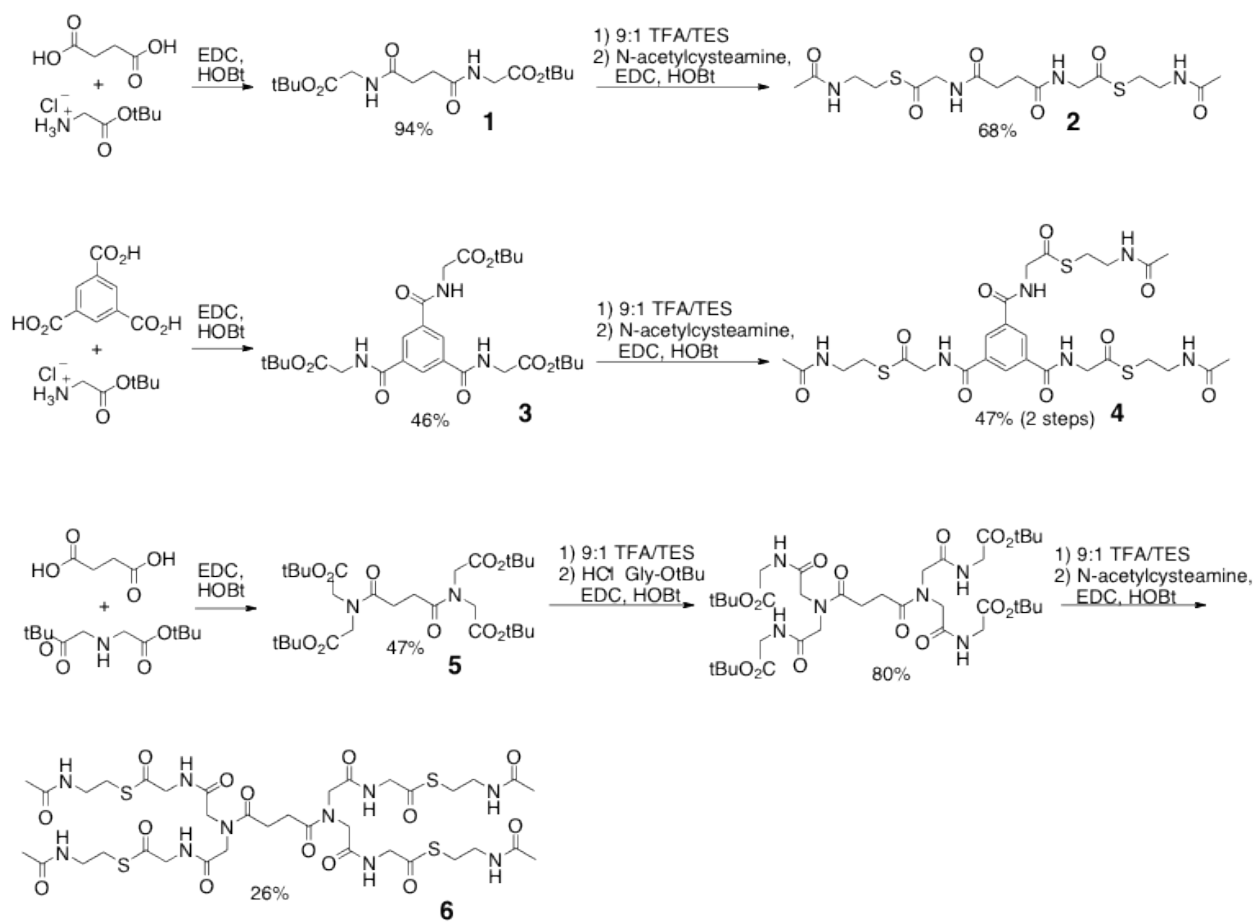


Figure S1. Synthetic routes used to prepare the thioester-modified scaffolds required for peptide conjugation.

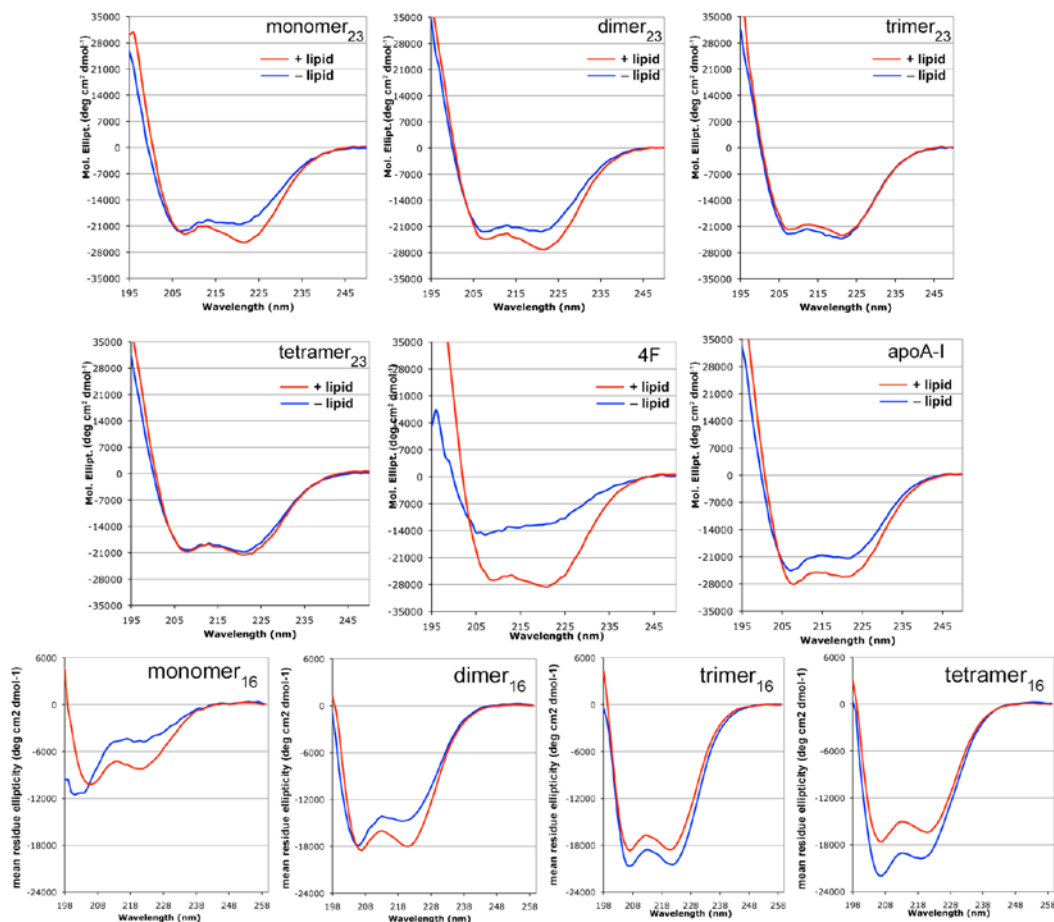


Figure S2. Circular dichroism (CD) spectra for the multivalent apoA-I mimetics as free peptides (blue lines) or as SEC-purified peptide nanoparticles (red lines) in PBS buffer, pH 7.4. The lipid/peptide mixing ratio was 10:1 for monomers, 20:1 for dimers, 30:1 for trimers, and 40:1 for tetramers. CD studies were performed to characterize the folding of the various peptide constructs in the absence of DMPC or in the context of nanoparticles. The 16-mer multivalent peptide constructs exhibited a higher degree of helicity, as judged by the magnitude of the minima at 222 nm, than the monomeric peptide in the presence or absence of lipid. The monomers and dimers exhibited increased helicity in the presence of lipid, as is typical of amphiphilic α -helical peptides. On the other hand, the trimers and tetramers were either unchanged or were somewhat less helical in the presence of lipid, suggesting that the lipid-free structures are fully folded due to intramolecular interactions.

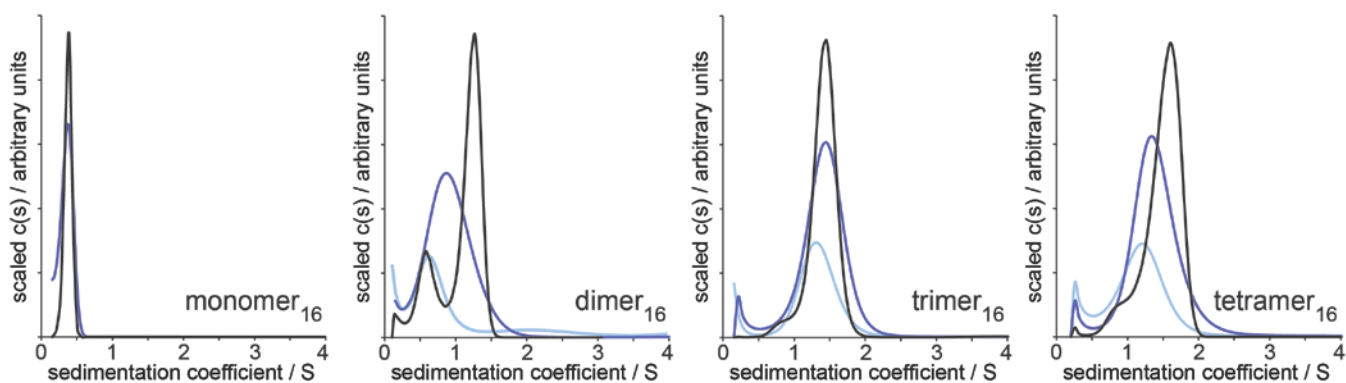


Figure S3. Sedimentation coefficient distributions $c(s)$ from sedimentation velocity studies of the lipid-free 16-mer multivalent apoA-I mimetic constructs. Shown are the scaled distributions for the samples at high concentration (black, 52–210 μ M), mid concentration (blue, 7–24 μ M), and low concentration (light blue, 0.7–2.0 μ M) (actual sample concentrations are given in Table S1). The observed $c(s)$ distributions for the multivalent constructs, having broad, concentration-dependent peaks, are indicative of reversible self-association occurring rapidly on the timescale of the sedimentation.^{S2} In contrast, the monomeric peptide appears not to self-associate at the concentrations tested. For each multivalent construct, the range of observed $c(s)$ peaks are within sedimentation coefficient values that would be expected for a molecular dimerization.

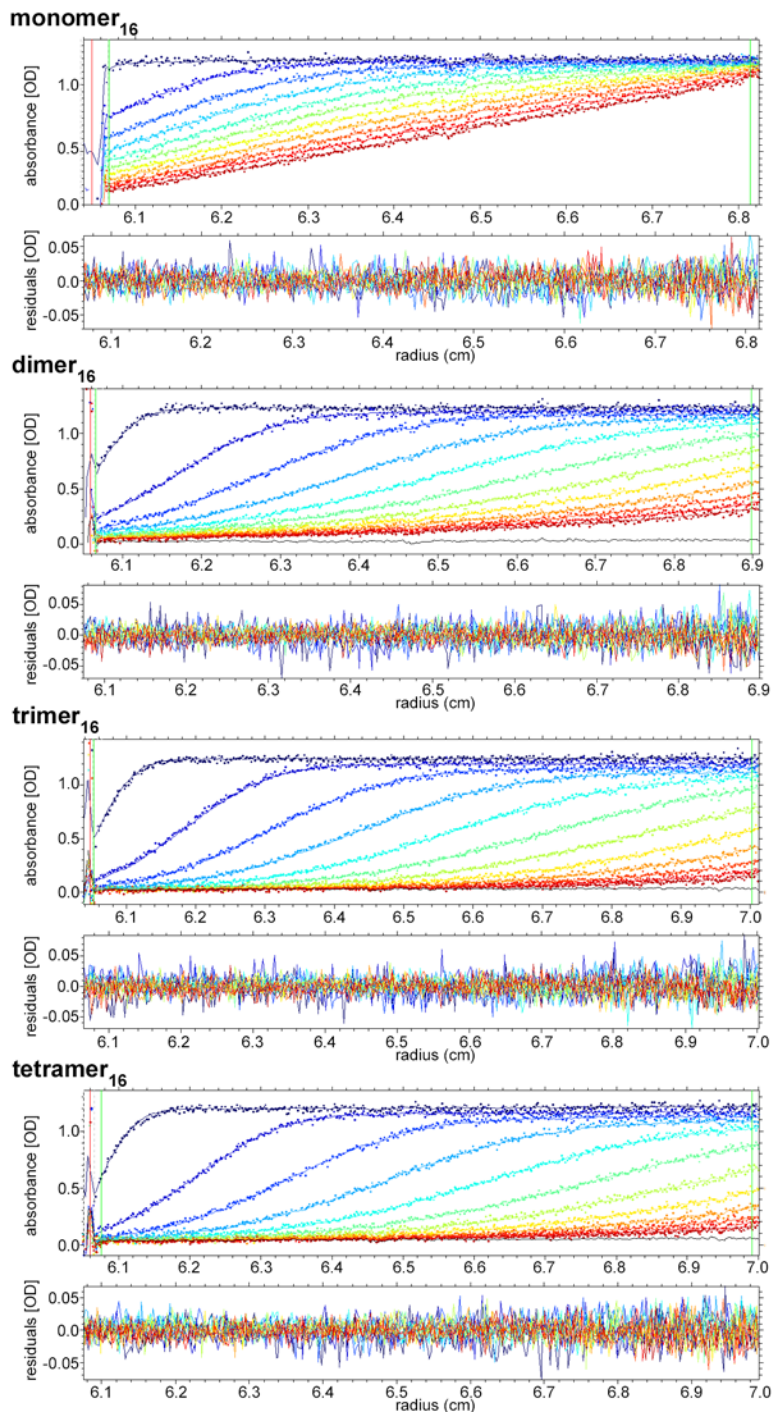


Figure S4. Sedimentation velocity profiles for each peptide construct, showing every 6th scan for the highest concentration sample. The solid lines represent the best fits of the data to the 'continuous $c(s)$ distribution' direct boundary model in SEDFIT v.13.0b. The data fit well to the model, as judged by the randomness of the residuals. The resulting $c(s)$ distributions are shown in Figure S4.

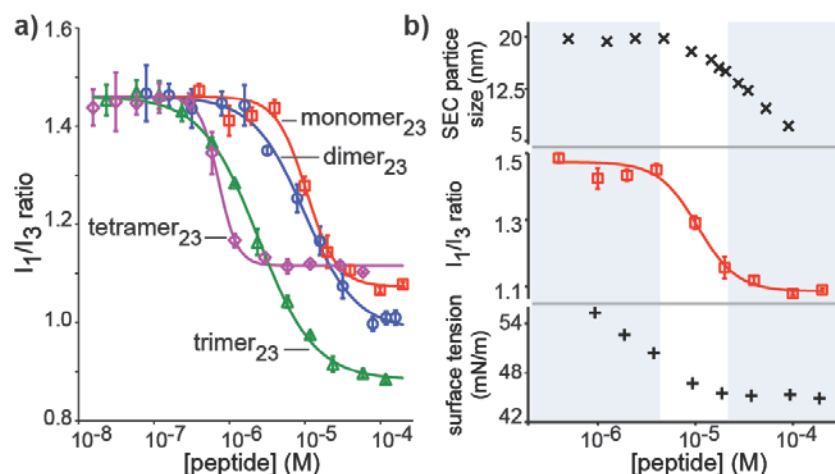


Figure S5. Congruence between peptide self-association and nanoparticle assembly equilibria. (a) Self-association of lipid-free 23-residue peptides were determined using pyrene fluorescence I_1/I_3 ratio measured at various peptide concentrations. Data are shown as the mean \pm SD of samples in triplicate. Curves are merely to guide the eye. (b) The transition concentrations in the monomer₂₃ self-association measurement (middle) correspond well with transition points in measurements of surface tension (bottom) and SEC analyses of nanoparticle size (top).

Because peptide self-assembly likely impacts the equilibria governing nanoparticle formation and dynamics,^{S6} we characterized the self-association concentration range for each of the peptides using pyrene fluorescence measurements over a range of peptide concentrations. Pyrene is a hydrophobic molecule with a low aqueous solubility and is solubilized in the hydrophobic domains of molecular aggregates. The fluorescence spectrum of pyrene is related to its vibronic fine structure, and the relative peak intensity is strongly dependent on the polarity of the microenvironment. With increasing polarity, the intensity of the first band (I_1) is enhanced, whereas no effect is observed on the intensity of the third band (I_3). Thus, the ratio of the I_1/I_3 bands in the pyrene fluorescence spectrum is sensitive to the polarity of the microenvironment and can be used as an indicator of self-assembly of amphiphilic molecules.^{S1a} As expected, the initially high pyrene I_1/I_3 ratio (reflecting a polar environment) decreased and eventually stabilized with increasing peptide concentration. Going from the monomeric peptide to the tetrameric construct, the observed self-association transitions occurred at lower concentrations. Clearly, the tetrameric peptide had the highest propensity for self-assembly, while the monomer had the lowest. Interestingly, the lowest peptide concentration at which self-association was observed (by pyrene fluorescence) matched the lowest peptide concentration at which nanoparticles were observed to form (by SEC) (Figure 3b), indicating that peptide self-association and lipid binding are related by similar biophysical driving forces.^{S6} The different plateaus in the higher concentration region of the pyrene fluorescence plot indicate that the self-associated complexes for each peptide have a different degree of nonpolar regions, to which pyrene can bind. Thus, the trimer complex apparently has a higher capacity to bind pyrene than the monomer complex, leading to a more nonpolar microenvironment and a lower I_1/I_3 ratio.

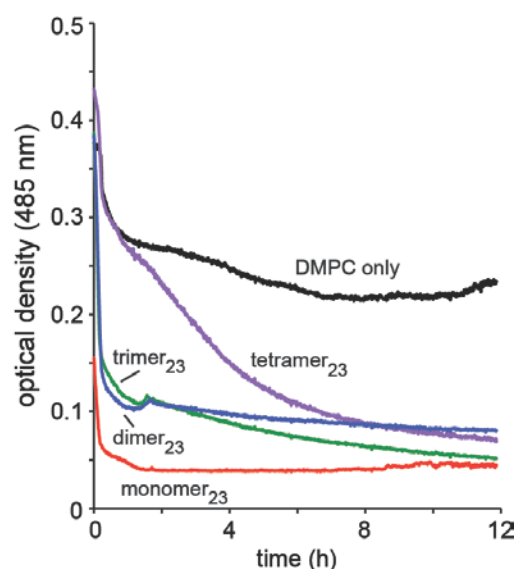
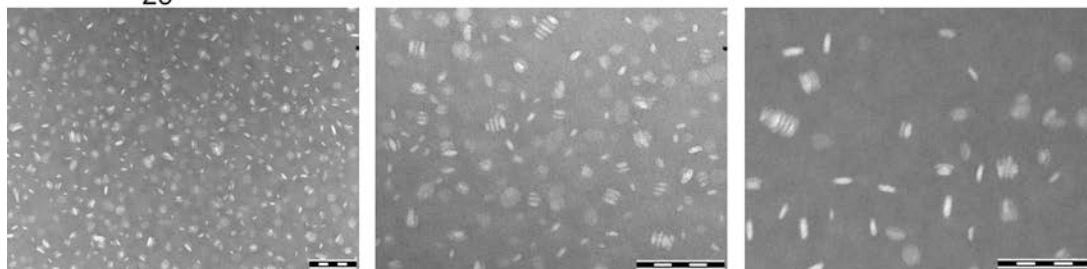
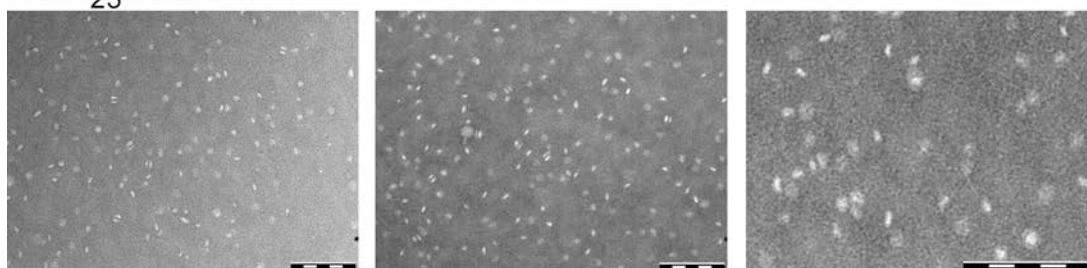


Figure S6. Liposome clearance assay. The peptide constructs were added to turbid suspensions of DMPC multilamellar vesicles at time 0. The kinetics of liposome remodeling into smaller nanoparticles (which do not scatter light) was monitored by recording the change in optical density over time.

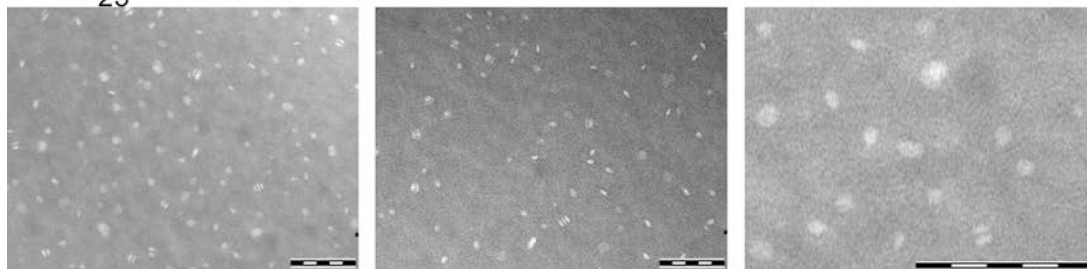
Monomer₂₃:DMPC 1:10



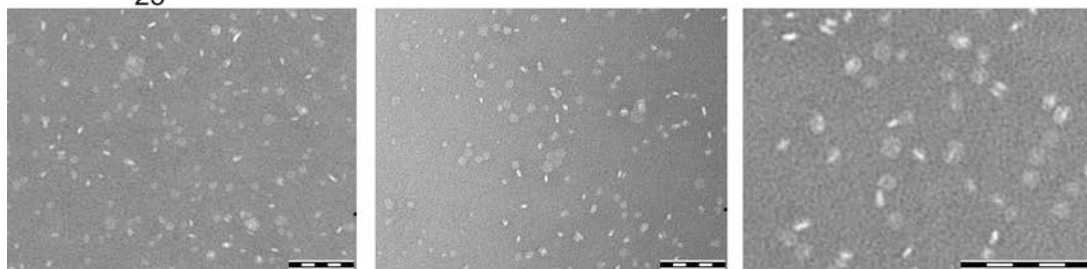
Dimer₂₃:DMPC 1:20



Trimer₂₃:DMPC 1:30



Tetramer₂₃:DMPC 1:40



apoA-I:DMPC 1:100

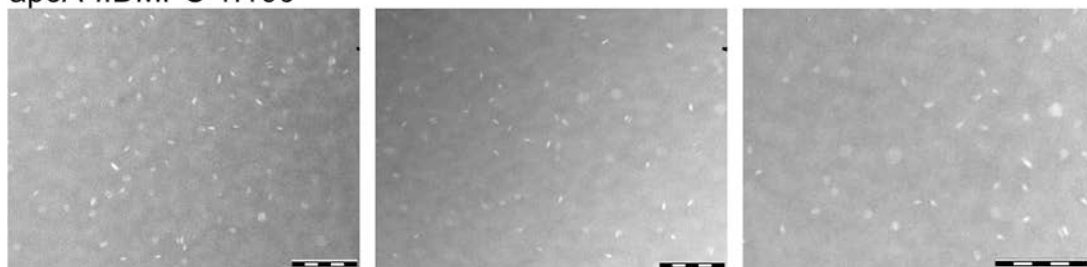


Figure S7. TEM images of nanoparticles prepared using the 23-mer peptide constructs. In all images, the scale bar represents 100 nm.

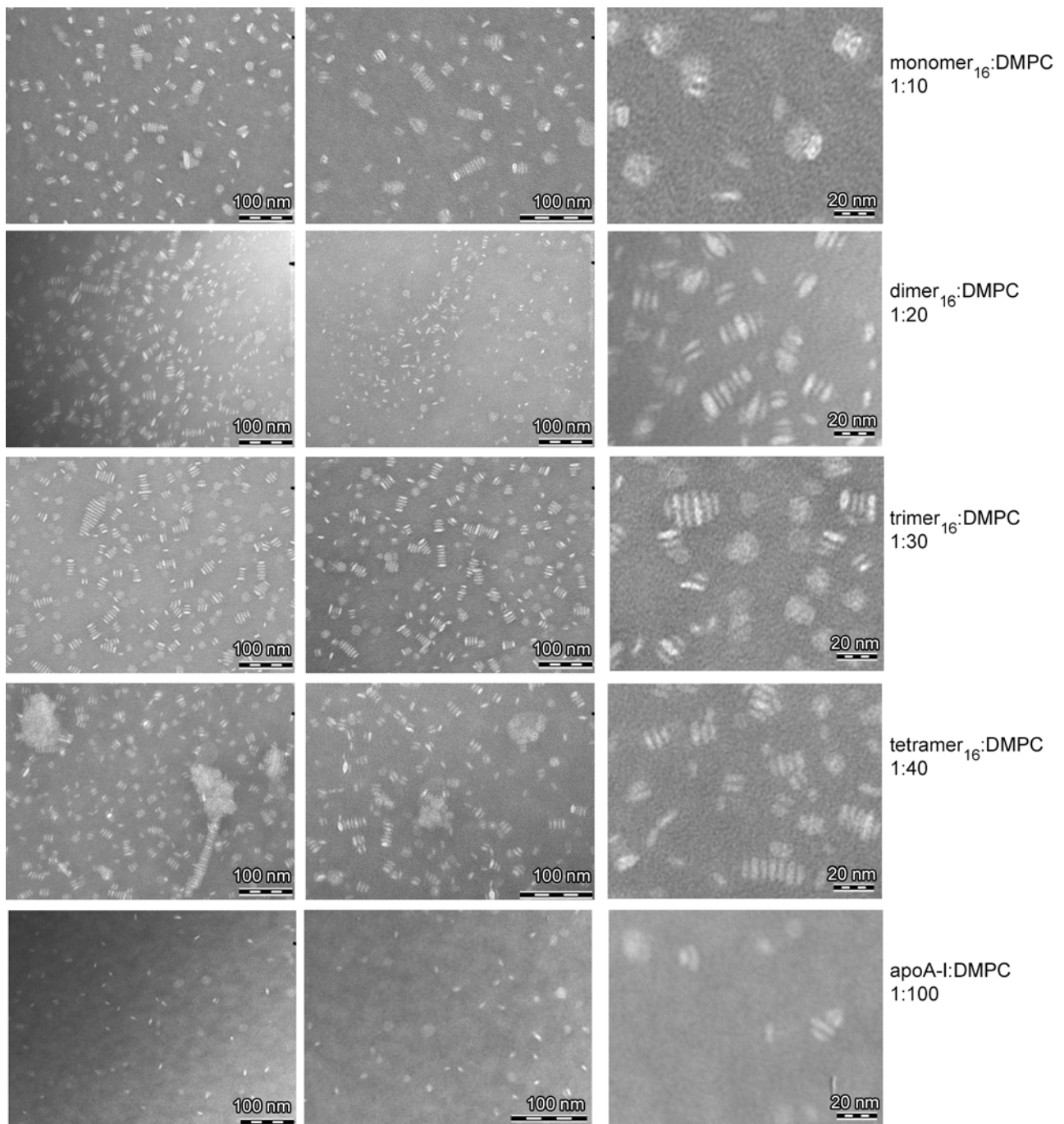


Figure S8. TEM images of nanoparticles prepared from 16-mer peptide constructs and human apoA-I.

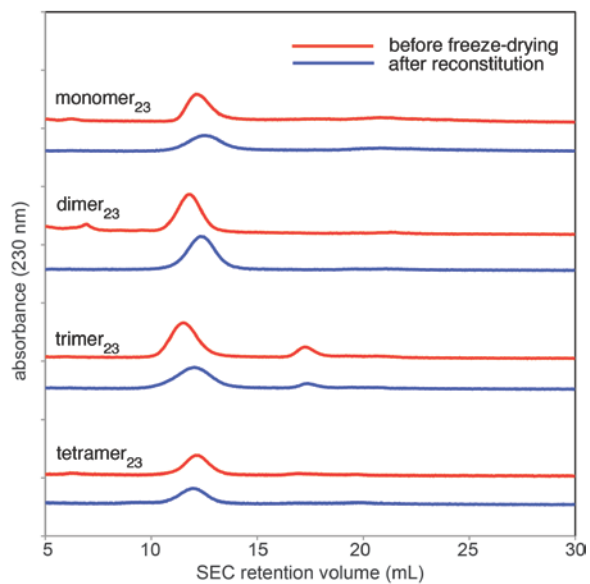
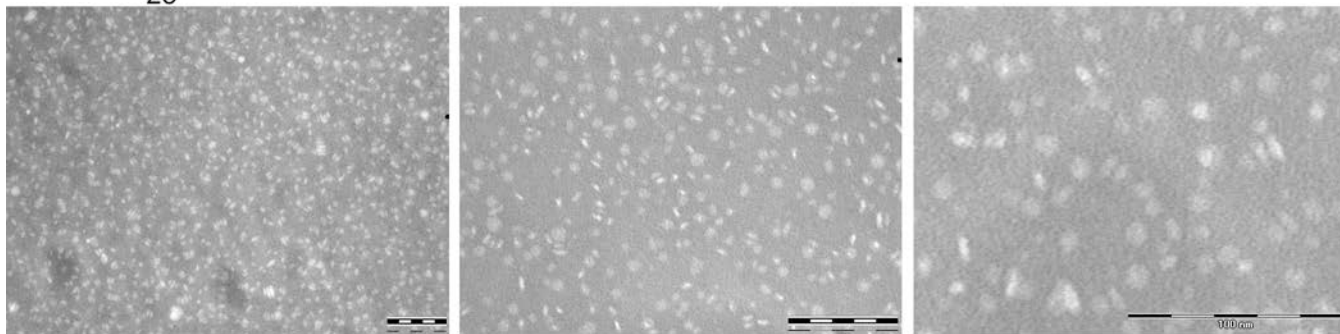
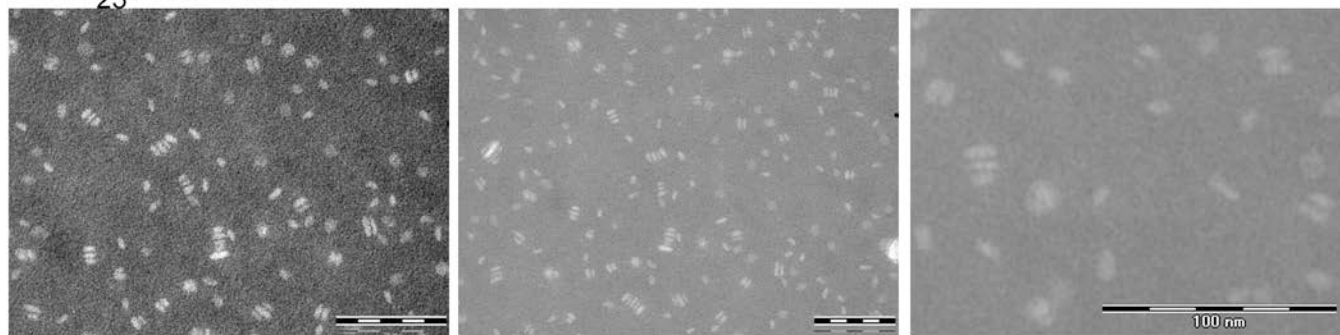


Figure S9. Size exclusion chromatography (SEC) profiles before freeze drying the 23-mer nanoparticle preparations (red curves) and after reconstitution by adding water (blue curves). For each construct, SEC and TEM analysis indicated that the reconstituted nanoparticles adopted similar size and morphology to freshly prepared ones.

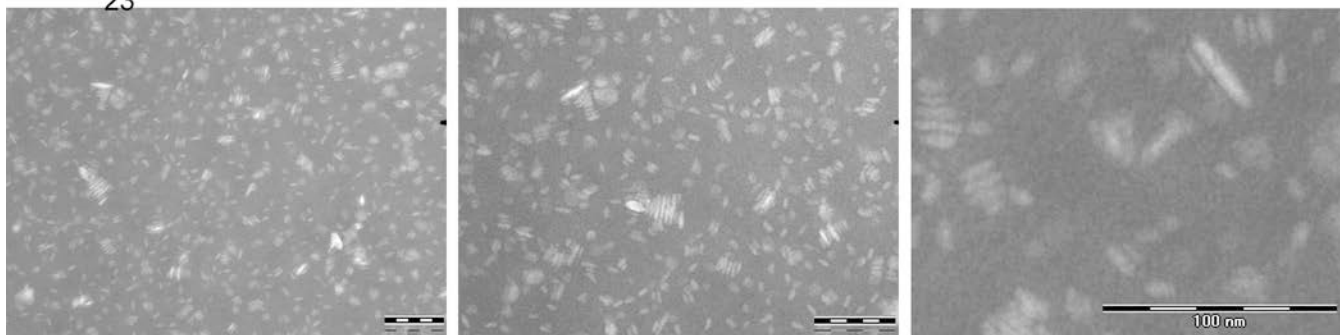
Monomer₂₃:DMPC 1:10



Dimer₂₃:DMPC 1:20



Trimer₂₃:DMPC 1:30



Tetramer₂₃:DMPC 1:40

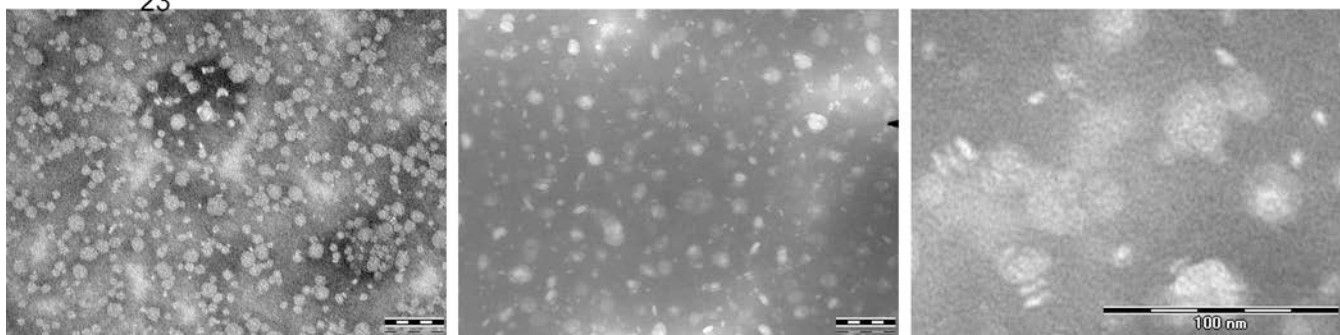


Figure S10. TEM images of nanoparticles that were freeze-dried and then reconstituted with water prior to TEM analysis. In all images, the scale bar represents 100 nm.

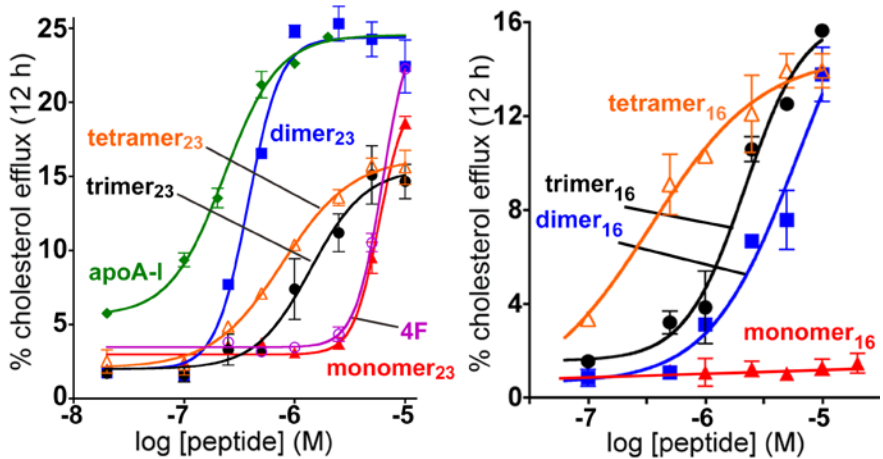


Figure S11. Multivalent apoA-I mimetic constructs efficiently promote cellular cholesterol efflux. Efflux was measured with cholesterol-laden mouse macrophage J774 cells over 12 h for the 23-mer series and the 16-mer series of lipid-free peptides, or lipid-free apoA-I. Values are shown as mean \pm SD of samples in triplicate. The peptide concentrations (μ M) at half-maximal efflux (EC_{50}) were: monomer₂₃, 5.8 ± 1.2 ; dimer₂₃, 0.4 ± 0.1 ; trimer₂₃, 1.4 ± 0.4 ; tetramer₂₃, 0.8 ± 0.1 ; 4F, 6.2 ± 1.3 ; apoA-I, 0.2 ± 0.1 ; monomer₁₆, >150 ; dimer₁₆, 6.2 ± 0.2 ; trimer₁₆, 2.2 ± 0.8 ; and tetramer₁₆, 0.3 ± 0.2 . On an efflux-per-molecular weight basis, dimer₂₃ is superior to apoA-I.

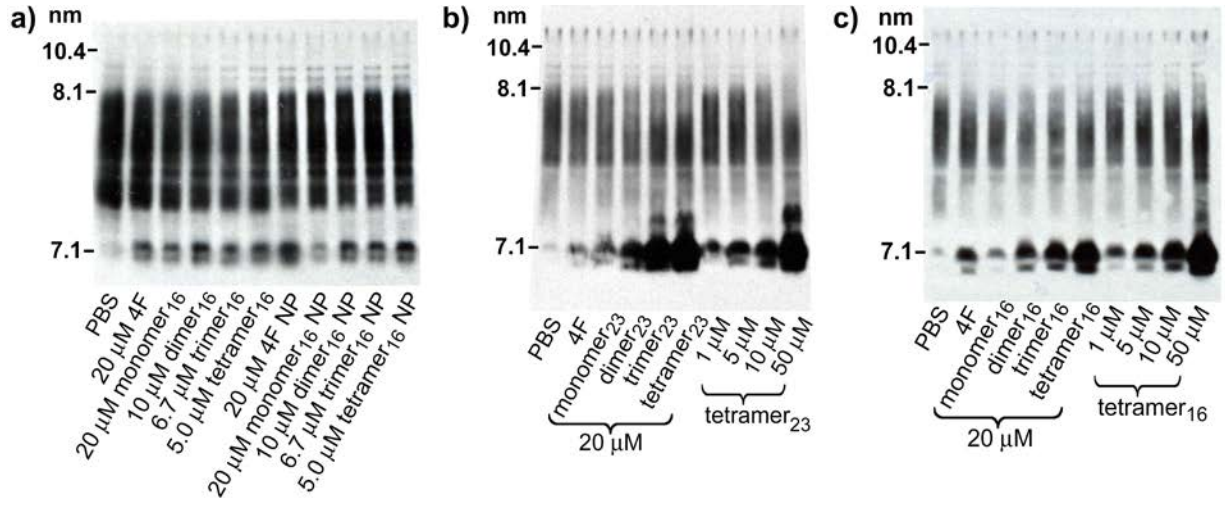


Figure S12. Remodeling of human plasma HDLs mediated by peptides and lipid nanoparticles (NP). Shown are Western blots for human apoA-I. The small, dense HDL particles around 7 nm are atheroprotective because they absorb and transport cholesterol away from peripheral tissues in RCT. 4F is a well-studied monomeric 18-residue apoA-I mimetic peptide.

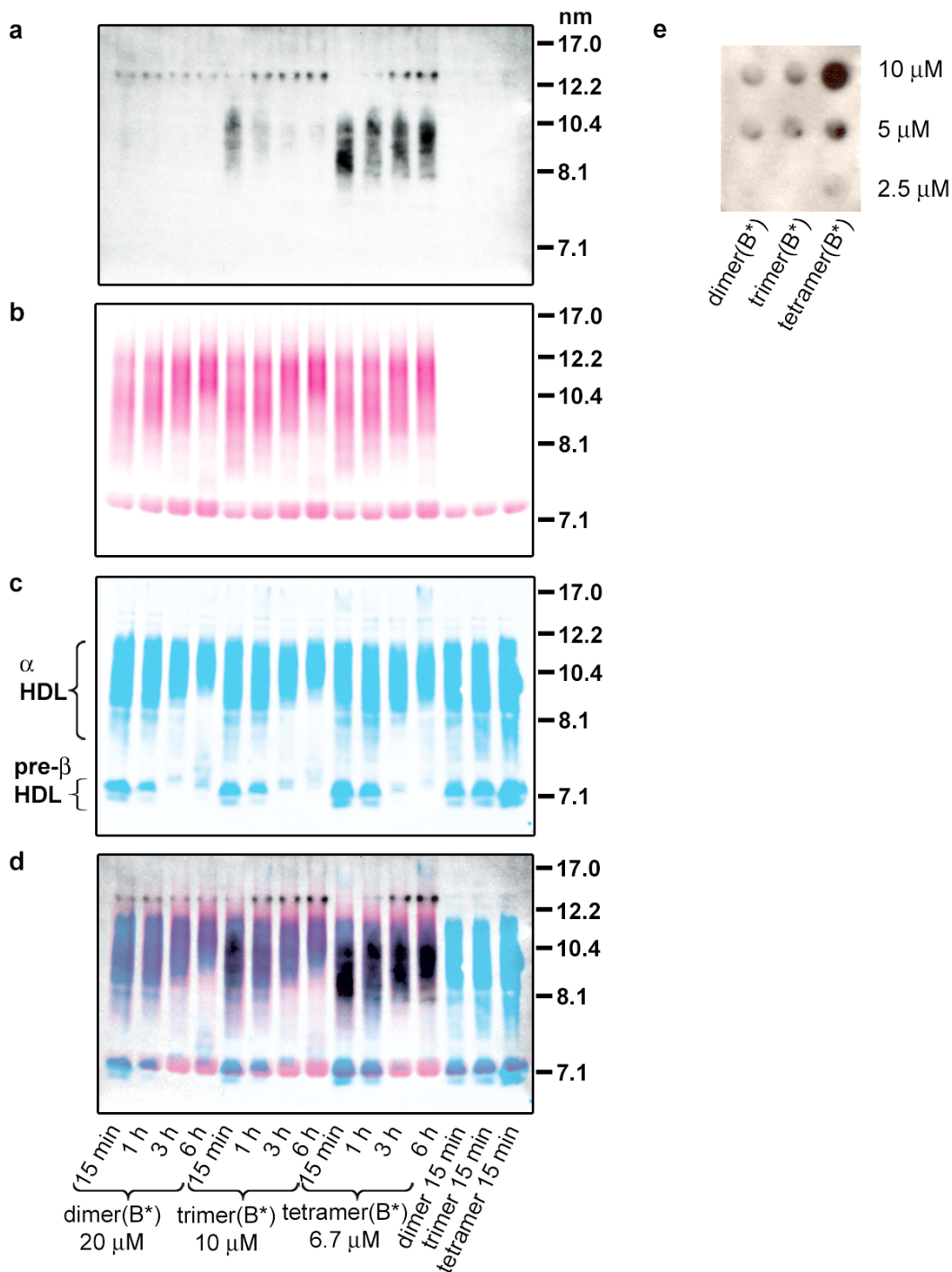


Figure S13. Tracking interactions between nanoparticle components and native HDLs with fluorescently labeled components for the 16-mer family of constructs. Lipid nanoparticles were formed from biotinylated 16-mer peptide constructs denoted by (B*) (black signal, panel a) and 1% rhodamine-labeled lipid (magenta signal, panel b). The particles were incubated with human plasma for various times, after which the samples were separated by NDGGE and fluorescently imaged. The band at 7.1 nm corresponds to human albumin, which autofluoresces and likely also binds labeled lipid to some extent. The last three lanes are nanoparticles generated with unlabeled peptides and lipid. The gel was Western blotted for biotin with HRP-NeutrAvidin to visualize biotinylated peptides (panel a); or c) Western blotted for apoA-I, indicating where native HDL particles are present. d) Overlay of the fluorescence images and the western blots. e) Dot blots of dimer₁₆(B*), trimer₁₆(B*), and tetramer₁₆(B*) nanoparticles at 10, 5, and 2.5 μM concentrations of helices (the same number of biotin moieties are present for each sample at a given concentration). Note that the blotting efficiency follows the trend of tetramer₁₆ > trimer₁₆ > dimer₁₆, likely due to differences in peptide absorption to the PVDF membrane. The rightmost three lanes in the gel do not contain any labeled materials, so the observed fluorescence in panel b can be ascribed to autofluorescence of serum albumin.

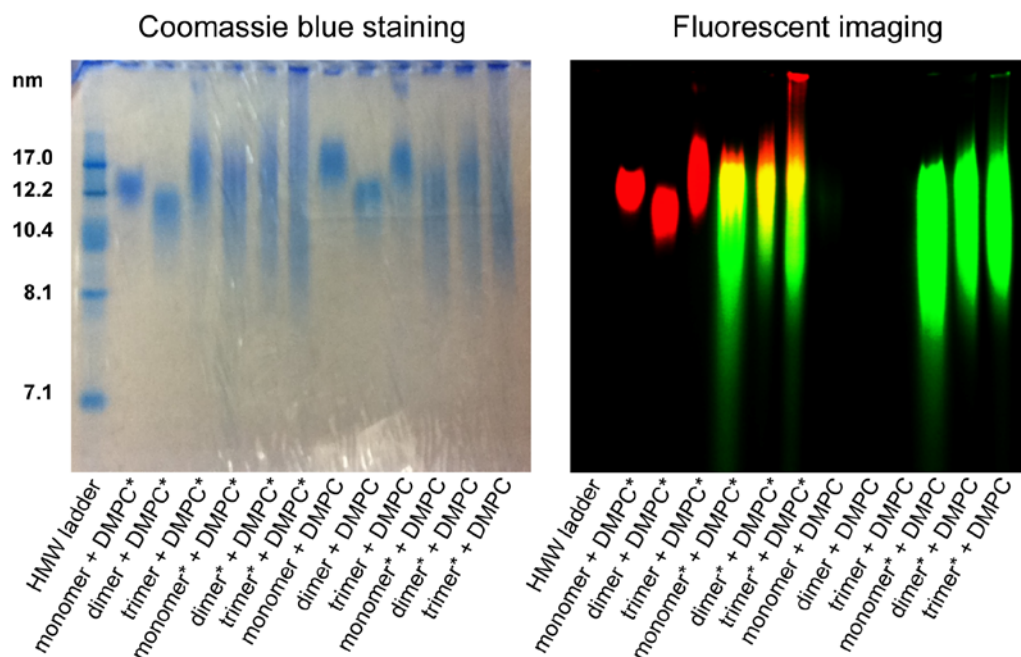


Figure S14. Characterization of lipid nanoparticles generated from fluorescently labeled 23-mer peptide constructs and lipid by NDGGE. Nanoparticles were formed using all possible combinations of labeled (*) or unlabeled peptide or lipid for the monomer₂₃, dimer₂₃, and trimer₂₃ peptide constructs. The nanoparticles were then run on a 4–20% native polyacrylamide gel, imaged on a fluorescent scanner, and then stained with Coomassie Blue. Green fluorescence represents labeled peptide, while red fluorescence represents labeled lipid. The nanoparticles assembled from labeled peptides exhibit a somewhat increased size distribution compared to unlabeled peptides.

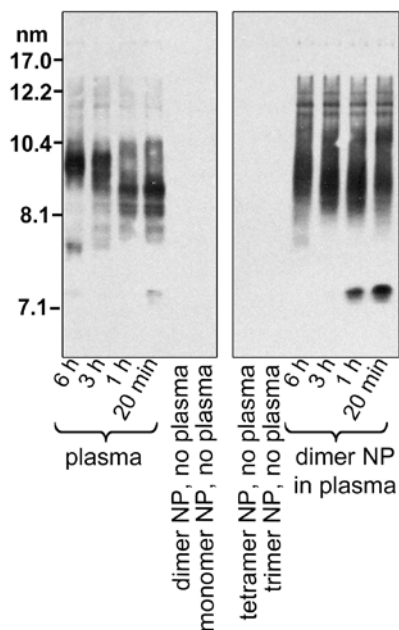


Figure S15. Confirmation that the antibody used to detect human apoA-I for Western blots does not bind to any of the 23-residue multivalent constructs. Signal is observed only in the lanes containing apoA-I from plasma.

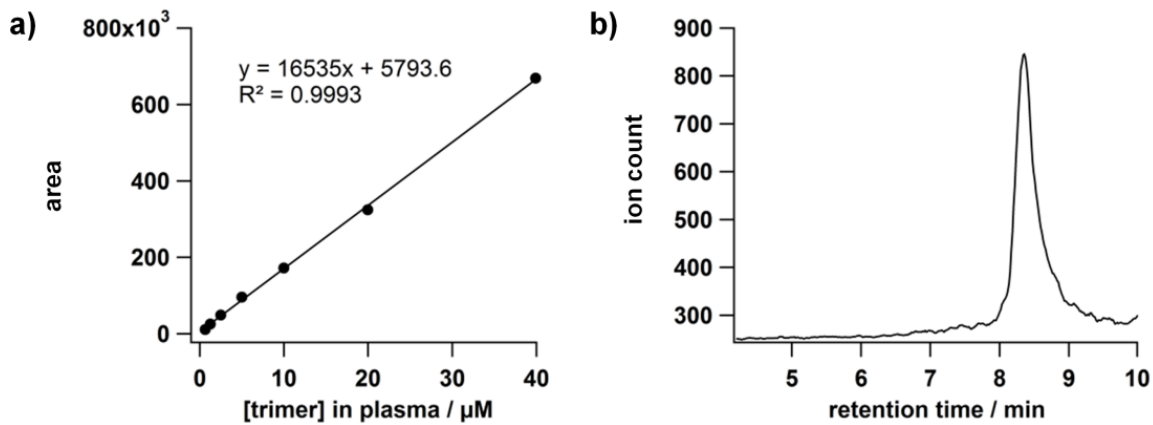


Figure S16. Determination of peptide concentration in plasma using HPLC/MS SIM. a) Representative calibration curve of trimer₁₆ construct in mouse plasma; b) representative selected MS ion trace (1504.7 [M+4H]⁴⁺) at trimer concentration of 0.6 μM (lower limit of detection) in mouse plasma.

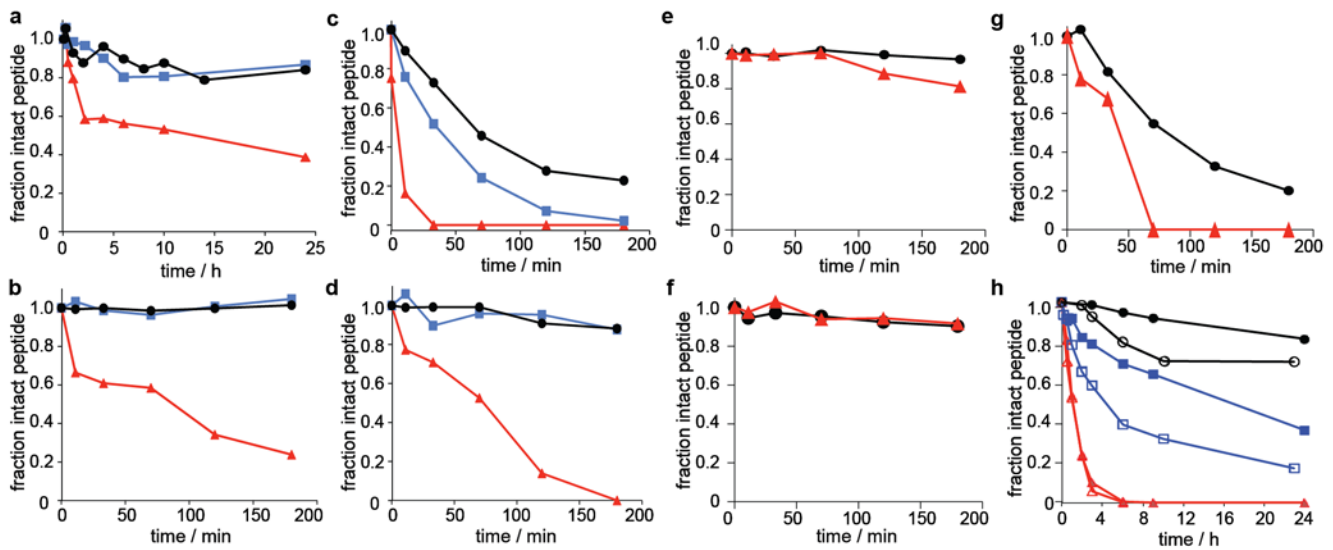


Figure S17. Susceptibility to proteolysis in vitro for 23-mer free peptides and peptide/DMPC nanoparticles. Monomer₂₃ (red triangle), dimer₂₃ (blue square), and trimer₂₃ (black circle) free peptides were incubated at 37 °C in PBS (pH 7.4) with a) mouse serum or 20 mU/mL proteases, b) chymotrypsin, c) pronase or d) thermolysin. Likewise, monomer nanoparticles and trimer nanoparticles were incubated at 37 °C in PBS (pH 7.4) with 20 mU/mL proteases, e) chymotrypsin, f) thermolysin, or g) pronase. Peptide concentrations were 0.1 mg/mL and 0.5 mg/mL in serum and protease incubations, respectively. Aliquots of serum or protease samples were removed and subjected to MeCN precipitation or protease inhibition (Complete™), respectively. The disappearance of peptide was monitored by LC/MS SIM. Panel h shows degradation of the lipid-free peptides (solid symbols) and peptide nanoparticles (open symbols) by pepsin (0.5 U/mL) at pH 2.2.

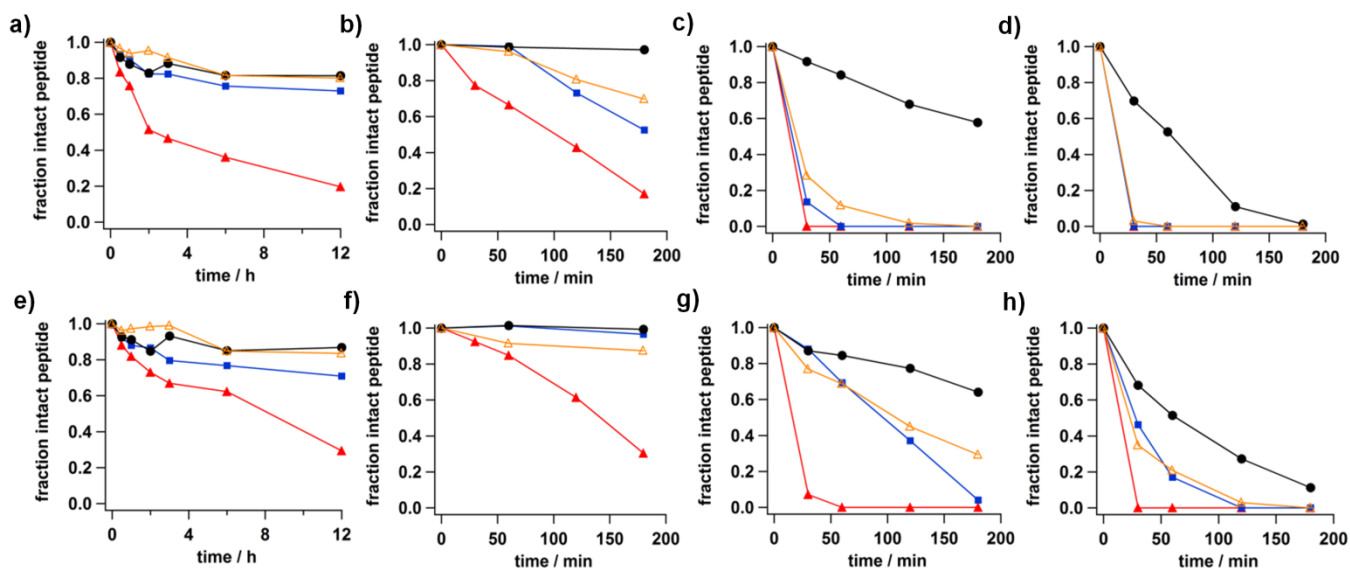


Figure S18. Susceptibility of 16-mer free peptides (a-d) and peptide lipid nanoparticles (e-h) to proteolysis in vitro. Monomer₁₆ (red triangle), dimer₁₆ (blue square), trimer₁₆ (black circle), and tetramer₁₆ (orange triangle) materials were incubated at 37 °C in PBS (pH 7.4) with (a,e) mouse serum or 20 mU/mL proteases (b,f) chymotrypsin, (c,g) thermolysin, or (d,h) pronase. In all cases, the monomeric peptide was least stable, and the trimeric peptide was the most stable. Peptide concentrations were 0.1 mg/mL and 0.5 mg/mL in serum and protease incubations, respectively. To quench the reactions, at various times aliquots of the serum or protease samples were removed and subjected to MeCN precipitation or protease inhibition (Complete™), respectively. The concentration of intact peptide remaining was determined by using LC/MS SIM.

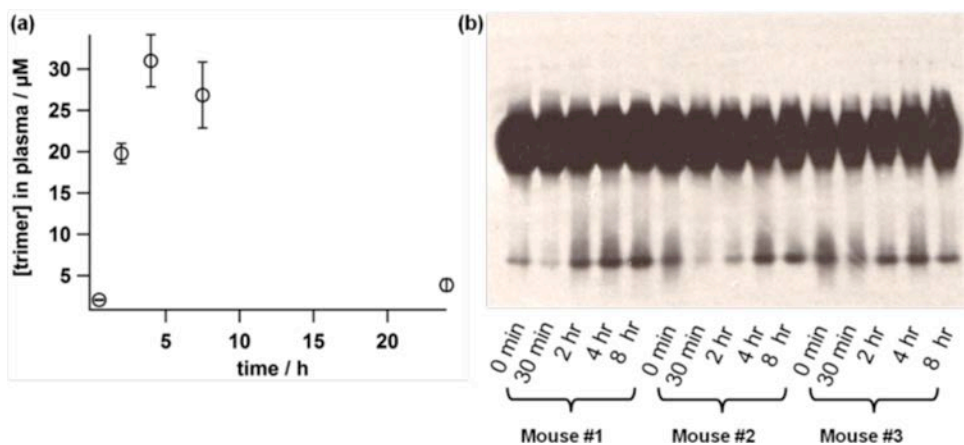


Figure S19. Pharmacokinetics and in vivo plasma HDL remodeling properties of trimer₂₃/DMPC nanoparticles in mice (*BALB/cByJ*, $n = 3$) by subcutaneous (s.c.) injection. (a) Mice were injected s.c. with a 90 mg/kg dose of trimer₂₃/DMPC nanoparticles. Blood was collected at 30 min to 24 h post-injection, and subjected to analysis by LC-MS SIM to determine the concentration of peptide present. Data are shown as mean ± SD. (b) Plasma samples from the PK study were western blotted for apoA-I.

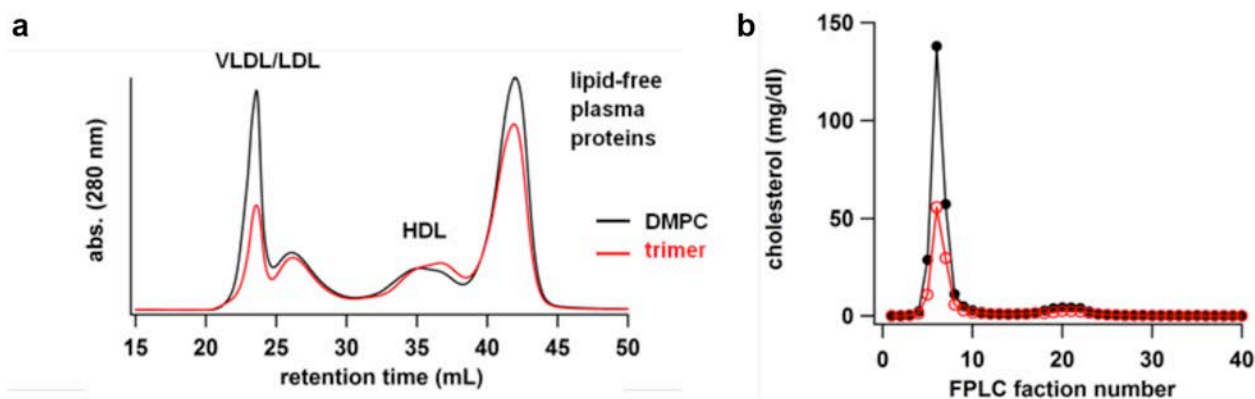


Figure S20. Lipoprotein profile analyses for LDLr-null mice treated daily (i.p.) for two weeks with DMPC liposomes or trimer₂₃/DMPC nanoparticles. Pooled plasma from all mice in each group was fractionated via FPLC. Inspection of the (a) absorbance (280 nm) trace or the (b) cholesterol trace indicated that the majority of total cholesterol reductions observed for the trimer₂₃ group are due to decreases in the VLDL and LDL levels. Although HDL levels are comparable for both groups, the HDL particles in the trimer-treated group have undergone a modest shift to smaller (later eluting) particles compared to DMPC control.